THERMAL AND MAGNETIC PROPERTIES OF LIQUID He³ AT LOW PRESSURE AND AT VERY LOW TEMPERATURES*

W.R. ABEL, A.C. ANDERSON, W.C. BLACK, and J.C. WHEATLEY

*Department of Physics and Materials Research Laboratory
University of Illinois, Urbana, Illinois*

Abstract

A brief review of the experimental and theoretical properties of low pressure liquid He³ as related to the present work is given. This is followed by a discussion of the magnetic cooling method as applied to cooling He³ using both nuclear and electronic paramagnetics. A number of possible metals for nuclear cooling are suggested, while cerium magnesium nitrate (CMN) is taken to be the best electronic paramagnetic known for the present purposes. The spin-bath thermal resistance is discussed in both cases. In the case of CMN recent work on the spin-bath resistance, due to a phonon bottleneck, shows it to be remarkably low. This is borne out in the present experiments. It is concluded that for temperatures in the millidegree range CMN is the best possibility.

A careful discussion is given of the techniques developed for obtaining and maintaining temperature below 0.010°K for many hours in an apparatus of moderate size using superconducting magnets. Details are given of the method of using epoxy resins for producing apparatus for using He³ with application to the measurement of heat capacity and magnetic properties. The method of executing the experiments is presented together with a thermodynamic analysis of the effectiveness of the final cooling process.

New measurements of the heat capacity of a mixture of low pressure He³ and CMN are presented down to a magnetic temperature of 0.004°K. No anomalous results are obtained. The experimental technique is analyzed and criticized. The results are compared with earlier data. The limiting value of C/nRT still cannot be precisely assessed but seems to be in the range 3.0 to 3.2°K^{-1}. Detailed comparison is made of the present work with that of Peshkov, whose results are interpreted in terms of an experimental effect. The thermal boundary resistance from epoxy walls to He³ compares favorably with previous work.

Measurements by the spin-echo method of the self-diffusion coefficient, D, and the susceptibility, χ, of the He³ are presented down to a temperature of 0.0035°K No anomalous behavior is observed. D obeys the law $D = 1.36 \times 10^{-6}T^{*-2} cm^2K°^2sec^{-1}$. to below 0.005°K. If an experimental effect is corrected for, χ appears to be temperature independent. Assuming that D defines the Kelvin temperature by $T \propto D^{-\frac{1}{2}}$,

the present work measures χ vs T without recourse to an auxiliary thermometer. The same assumption leads to the conclusion that the Kelvin and magnetic temperatures differ by only 0.0001°K at 0.0035°K. The He^3 spin-lattice relaxation time, measured down to 0.004°K where it is about 2 sec in the present cell, decreases with decreasing T but without a well defined temperature dependence.

1. INTRODUCTION

SOME years ago L.D. Landau [1] developed a phenomenological theory of Fermi liquids and suggested that the theory would be applicable to liquid He^3 at sufficiently low temperatures. The nucleus of the He^3 atom has spin one-half, and the atoms do not bind together to form molecules. Hence it was assumed that at sufficiently low temperatures, in spite of the very strong interactions in the liquid, the excitations of importance would be quasiparticles which obey the Fermi distribution law. The lifetime of these quasiparticle excitations would be limited only by collisions with one another since there is no other scattering mechanism. Considering the collisions of a given particle, the number of quasiparticles against which it can scatter will be proportional to the absolute temperature, T, and the number of allowed final states will also be proportional to T so that the collision frequency will be proportional to T^2. For the theory in its simplest form to be valid, the quasiparticles should be defined at least as well as the energy kT, and since the quantum uncertainty in the energy of the quasiparticles due to collisions will be proportional to T^2, there should be some temperature below which the simple considerations of the theory are valid. Landau's original theory has been amplified and detailed calculations for He^3 made by Abrikosov and Khalatnikov [2] and by Hone [3], among others. It is found that the thermal conductivity should be proportional to $1/T$, that the viscosity should be proportional to $1/T^2$, that the self-diffusion coefficient for the magnetization should be proportional to $1/T^2$, that the specific heat should be proportional to T, and that the nuclear magnetic susceptibility and the velocity of ordinary hydrodynamic sound should be independent of T. Landau also predicts [4] a collective motion of the quasiparticles which is like a sound wave but which is fully developed only in the case in which there are no collisions between the quasiparticles. This motion corresponds to an oscillation of the Fermi surface and was called by him "zero sound". Zero sound waves are very difficult to measure using ordinary techniques because of the very short attenuation length. Abrikosov and Khalatnikov find [2] that a zero sound wave is attenuated to $1/e$ of its original amplitude in a distance equal in magnitude to the velocity of zero sound multiplied by the collision time; hence the zero sound wave is attenuated in a distance of the same order of magnitude as the quasiparticle mean free path. Since only at very low temperatures is the quasiparticle mean free path large on a laboratory scale, one expects that only at very low temperatures will measurements of the characteristics of zero sound using a pulse experiment or a resonance experiment be possible. It is also necessary for the observation of zero sound that the product $\omega\tau$ be very much greater than unity, where ω is the angular frequency of the sound, and τ is the collision time.

Another phenomenon of importance for liquid He^3 is the very high thermal boundary resistance between the liquid and an adjacent solid body [5,6]. This resistance is of importance for all experiments on liquid He^3 at low temperatures since, in order to cool the He^3, heat must be transferred either through the walls of the container or into the grains of a powdered refrigerant. Since the specific heat of the liquid is proportional to T and since the thermal conductivity is proportional to $1/T$, one expects that the thermal time constant of the liquid He^3 should be proportional to T^2. Hence the liquid itself may be expected to be homogeneous in temperature at low temperatures. Indeed, at sufficiently low temperatures the thermal time constants of most reasonable geometries turn out to be very small. On the other hand, heat is

transferred into the liquid He^3 from the surrounding walls by means of the mechanical vibrations of the walls exciting oscillations in the liquid. At very low temperatures the amplitude of vibrations of the walls is small, and consequently the rate of transfer of energy into the liquid is also small. The heat transfer process can be thought of in terms of the radiation of sound; hence it is not surprising that one finds that the heat flux through the wall is proportional to the difference in the fourth powers of the absolute temperatures of the walls and of the liquid helium. Assuming a uniform temperature in the walls one then finds that there is a temperature discontinuity at the interface between the solid and the He^3. This temperature discontinuity divided by the heat flux is defined to be the boundary resistance. For small temperature differences it is proportional to $1/T^3$. Thus the thermal time constant for liquid He^3 (heat capacity linear in T), in contact with its surroundings through the boundary resistance, will be proportional to $1/T^2$.

At very low temperatures the mechanical motion of the walls is expected to be transmitted directly into zero sound motion in the liquid. This expectation is supported by the experiments of Keen, Matthews, and Wilks [7], in which the walls were vibrated not thermally but by means of piezoelectric action. They found the effective acoustic impedance of He^3 to be different in the low temperature region from that in the high temperature region.

Several years after the work of Landau, it was suggested by a number of workers [8,9,10] that at a sufficiently low temperature the liquid He^3 would undergo a phase transition. The low temperature phase of He^3 is thought to consist of a highly correlated motion of quasiparticles similar to that suggested by Bardeen, Cooper, and Schrieffer [11] to explain the phenomenon of superconductivity. In the case of He^3, the quasiparticles with sufficiently large impact parameters attract one another by means of the van der Waals force, and the resulting highly correlated phase is thought to be made up of pairs of quasiparticles in such states. A number of detailed predictions on the properties of the highly correlated phase have been given, the transition profoundly influencing the properties of the liquid [12,13,14,15]. It is found for example, that at the transition temperature there should be a discontinuity in the specific heat of the He^3, that the susceptibility should decrease at the transition temperature, and that the transport coefficients should decrease sharply in the region of the transition. It was thought at one time [12,13] that the susceptibility would be affected only for pairing of even orbital angular momentum states, but recent work [16] shows that in relative p-states there is also a decrease in susceptibility. This result may be true in general.

Several years ago the technical difficulties involved in doing experiments with liquid He^3 at very low temperatures were partially overcome and it was possible to perform several different experiments. The heat capacity was measured to a temperature of 8 m°K (1 m°K $\equiv$ 10^{-3}°K) and found to be nearly linear in the absolute temperature below approximately 30 m°K [17]. The thermal conductivity was measured to a temperature of 30 m°K [18]. At temperatures between 30 m°K and 40 m°K the thermal conductivity was in agreement with a $1/T$ law, but did not define one. The viscosity was measured by ultrasonic attenuation to a temperature of 60 m°K [19]. Again the low temperature results were in agreement, within experimental scatter, with a $1/T^2$ law but did not define the law. The velocity of sound was found to be independent of temperature [19]. In the case of the magnetic measurements on He^3 [20,21], which were carried to a temperature of 22 m°K, it was found that Fermi liquid behaviour was rather well defined. The nuclear magnetic susceptibility of the He^3 was constant below 100 m°K and the self-diffusion coefficient for the magnetization was found to vary as $1/T^2$ (the 2 in the exponent was determined to 1 per cent) below about 40 to 50 m°K. In subsequent experiments it was found that the boundary resistance between solids and liquid He^3 varied as $1/T^3$ for temperatures less than 100 m°K [6]. Moreover, the measurements by Wilks and collaborators [7] of the attenuation by adjacent liquid He^3 of a longitudinally vibrating quartz rod strongly indicated the presence

of zero sound excitations in the liquid at sufficiently low temperatures [22,23]. Thus the experiments seem to show that He^3 at temperatures below 30 to 50 m°K and at low pressures is a Fermi liquid in the sense originally suggested by Landau, but it is also clear that measurements at much lower temperatures are necessary in order to determine definitively the Fermi liquid properties, to search for a direct confirmation of the phenomenon of zero sound, and to search for a temperature region in which the predicted highly correlated phase might be observed. It is the purpose of the present paper to present the results of a recent effort to make measurements at these reduced temperatures. The principal impediment to making progress in this area is essentially the technical one of lowering the temperature and maintaining it at a sufficiently low value. For that reason a substantial part of this paper will be devoted to some of the problems of refrigeration and isolation which must be overcome to obtain very low temperatures.

During the progress of the present experiments V.P. Peshkov in the U.S.S.R. reported [24] the discovery of superfluidity in He^3 by observation of a peak in the heat capacity of a mixture of He^3 and cerium magnesium nitrate at approximately 5 to 6 m°K. Some of the experiments to be described here are rather similar to those of Peshkov, both being similar to experiments performed in this laboratory in 1961 [17]. We now believe that the peak in the heat capacity measured by Peshkov is a spurious experimental effect. The results to be presented here show that there is no superfluidity in liquid He^3 to a temperature of about 3.5 m°K.

II. PRINCIPLES AND METHODS OF REFRIGERATION

In this section we consider cooling only by adiabatic demagnetization since there does not seem to be another method either as powerful or as easily effected. Down to temperatures of approximately 15 to 20 m°K one may consider the appropriate experimental techniques to be thoroughly worked out. A discussion of the method used and the type of results which can be expected is to be found in a paper by Anderson, Salinger, and Wheatley [25]. This work has recently been repeated in another connection and it was found that the earlier work was well reproduced [26]. A large number of experiments have been designed and performed based upon the general techniques described there and each has worked satisfactorily. Hence in the present paper one is concerned only with the methods and techniques useful for producing temperatures below 20 m°K.

Unfortunately, there seems to be no way to make a large change in the temperature of liquid He^3 by isentropic variation of some external parameter which affects the state of the He^3 itself. Hence the He^3 has to be cooled by some refrigerant placed in contact with it. For this reason the Kapitza thermal boundary resistance is always important. In practice two Kapitza resistances should be considered. The first one is the thermal boundary resistance between the outside walls of the container of the He^3, which we shall call the "cell", and the He^3 itself. This is the resistance through which the heat must flow to precool the He^3 to a temperature of approximately 15 to 20 m°K. The second thermal boundary resistance is that between the He^3 and a finely divided refrigerant with which it is mixed in order to perform the final cooling process. It is desirable to have the thermal resistance between the walls of the cell and the He^3 as large as possible consistent with the residual heat leak. If the residual heat leak is sufficiently small, and if one waits for a sufficiently long period of time, the cell and its contents will eventually come to a temperature close to that of the walls of the cell. After cooling the contents of the cell, they warm up through the thermal boundary resistance and, if the resistance is relatively large, as has been assumed, the rate of warming will be correspondingly low. One is, in this sense, using *time* as a thermal switch. In this connection it is worthwhile

to observe that the thermal boundary resistivity between He^3 and the walls of a cell constructed of copper wires and epoxy resin [6] is practically the same as the thermal boundary resistivity measured for the contact between copper wire coil-foil and slabs of chromium potassium alum (chrome alum) [25]. Of course, a very much larger area of contact is made with the chrome alum than with the He^3. It should be noted that the thermal boundary resistance between the cell wall and the He^3 as well as the thermal boundary resistance between chrome alum and coil-foil have been measured several times, and it appears that the experimental conditions leading to these resistances are readily reproduced.

The second thermal boundary resistance, that between the He^3 and the refrigerant with which it is mixed in order to perform the final cooling, should be as small as possible. For this reason the refrigerant should be finely divided and in intimate contact with the He^3. This resistance must be small in order that the thermal time constant of the system consisting of the He^3 and the refrigerant be as small as possible. Then less time will be required to make the adiabatic demagnetization process more closely isentropic.

In the temperature range under consideration there are two types of refrigerants to choose from; one is an electron paramagnetic and the other is a nuclear paramagnetic. In either case one observes that the spin-lattice resistance is in series with the Kapitza resistance and that the overall time constant is essentially the spin-bath relaxation time. With nuclear paramagnetics, one might expect the spin-bath relaxation time in metals to be sufficiently short at low temperatures to allow experiments to be performed.

The basic thermodynamic equation on which the cooling is based is

$$S_R(H_i, \ T_i) \ + S_3(T_i) \ = S_R(H_f, \ T_f) \ + S_3(T_f),   \tag{1}$$

where S is entropy, R is the refrigerant, 3 is the He^3, H and T refer to the magnetic field and the temperature, and i and f refer respectively to initial and final states. This equation is valid for isentropic cooling. Using the most recent values for the entropy of He^3 this equation may be rewritten

$$7 \times 10^6(T_i \ - \ T_f)V_3 \ \text{ergs/cm}^3 \ \text{K}^{\circ 2} \ = V_R[s_R(H_f, \ T_f) \ - \ s_R(H_i, \ T_i)],   \tag{2}$$

where V is volume and s_R is entropy of refrigerant per unit volume. Because of irreversibility this equation gives only the upper limit of the value of $(T_i \ - \ T_f)$ obtainable by adiabatic cooling. A choice between electronic and nuclear cooling certainly depends on whether or not the entropy change of the refrigerant in a magnetic field is sufficiently large. However, the choice also depends on whether the process of adiabatic cooling can be carried out reversibly in a sufficiently short time and, moreover, on the technical complications required to execute the process. The electronic and nuclear possibilities will be considered separately below.

In the case of nuclear adiabatic demagnetization there are a number of possibly useful metals. Assuming that the nuclei interact only with an external field, the spin entropy is given by the formula

$$S/nR \ = \ \ln(2I \ + \ 1) \ - \ 2/3 \ x^2 \ I(I \ + \ 1)   \tag{3}$$

where $x = g\beta H/2kT \ll 1$, I is the nuclear spin, g is the nuclear g-factor, β is the nuclear magneton, and k is Boltzmann's constant. The best species for nuclear adiabatic demagnetizations

are hence those with a large magnetic moment and a large spin. It is also important for the spin-lattice thermal resistance, as estimated below, to be small. The electric quadrupole splitting is in principle harmful but in the present application is not very serious since the external magnetic field will probably not be turned off completely. In any case, cubic metals are desirable to reduce the quadrupole splitting.

In metals there is also always the possibility of eddy-current heating. Assuming complete field penetration of the metal, the formula for the eddy-current heating of wires of diameter d with a superposed axial field B is, per unit volume,

$$\frac{\dot{Q}}{V} = \frac{1}{32} \sigma \dot{B}^2 d^2 \times 10^{-9} \; \frac{\text{erg sec ohm}}{\text{gauss}^2 \; \text{cm}^4}, \tag{4}$$

where σ is the conductivity. It is instructive to work out the heating rate per unit volume in the case of copper where one would expect to use wires of diameter 1.3×10^{-3} cm (No. 56 A.W.G.) and where the conductivity at low temperatures might be expected to be 4×10^7 ohm^{-1} cm^{-1} characteristic of a resistance ratio of 70, which seems to be typical of relatively fine magnet wire. The resultant eddy-current heating rate per unit volume is $2 \times 10^{-9} \dot{B}^2$ erg sec/gauss^{2}cm^3. Hence for relatively slowly varying external fields eddy-current heating is not likely to be a serious problem.

The properties of a number of metals which might possibly be useful for low temperature refrigeration are shown in Table 1. Platinum will evidently not be an outstanding refrigerant, but its short spin-lattice relaxation time T_1, makes it a possible thermometer. The metals except copper and platinum are all superconducting, but it is assumed here that the external field never goes below the critical field. Using equation (3) for the spin entropy, the entropy which may be removed from these substances on application of a field of 30,000 gauss at a temperature of 15 m°K has been calculated and is listed in Table 2. It is seen that in all cases, with the exception of platinum, the entropy removed per unit volume is substantial. Recalling that the entropy per unit volume of He^3 at low pressure is 1.05×10^5 ergs/cm^3°K at 15 m°K, one sees that in all cases except platinum one would expect a reasonable amount of cooling on adiabatic nuclear demagnetization, from this temperature, of a mixture containing roughly equal volumes of metal and He^3. Indeed in the case where the metals are in the form of fine wire it should be possible to have the volume of metal substantially greater than the volume of He^3. Thus nuclear cooling should be a sufficiently powerful tool using fields which are readily obtained from superconducting magnets.

Aside from purely entropic considerations, as noted above, one must also consider the thermal resistance between the spins and the He^3 bath. Consider the simple system of thermal reservoirs and thermal resistances shown in Fig. 1. In this figure S corresponds to the spin system, L corresponds to the "lattice", which in the case of a metal in a non-superconducting state would be the thermal bath of the conduction electrons, and 3 corresponds to the bath of He^3. R_{SL} corresponds to the thermal resistance between spins and lattice, and R_{L3} corresponds to the series combination of the thermal resistance of the "lattice" and the Kapitza resistance between the metal and the He^3. It is likely that at sufficiently low temperatures only the Kapitza resistance will be important in R_{L3}.

In what follows consider specifically the nuclear cooling case. R_{SL} is related to the nuclear spin-lattice relaxation time T_1. T_1 is usually measured under the experimental conditions that the heat capacity of L is very large compared with the heat capacity of S. In this case it is found experimentally that $T_1 = \beta/T$, where β is a constant. To relate T_1 and R_{SL} it is sufficient only to analyze the equilibrium between S and L in this case. Assuming then that

TABLE 1

Properties of metals possible for use in cooling by adiabatic nuclear demagnetization.
The natural isotopic abundance, Larmor frequency per unit field, nuclear spin I, and
quadrupole moment Q are taken from a table distributed by Varian Associates, Palo Alto,
California (publication No. INS 1522, fourth edition, 1964). Pt^{195} and solid He^3
are listed for comparison only.

Nucleus	Natural Abundance (%)	Larmor Frequency per Unit Field (kc/gauss sec)	$g\beta$ (10^{-24}erg/gauss)	I	(10^{-24}cm^2)	Crystal Structure	Molar Volume (cm^3/mole)	$T_1 T$ (sec °K)
Al^{27}	100	1.1094	7.35	5/2	0.149	f.c.c.	9.97	1.80 ± .05[a]
Cu^{63}	69.1	1.1285	7.48	3/2	−0.16	f.c.c.	7.1	1.27 ± .07[a]
Cu^{65}	30.9	1.2090	8.01	3/2	−0.15	f.c.c.	7.1	1.1[a]
In^{113}	4.16	0.9310	6.17	9/2	0.750	tet.f.c.	15.71	
In^{115}	95.84	0.9329	6.18	9/2	0.761	tet.f.c.	15.71	~ 0.1[b]
Nb^{93}	100	1.0407	6.90	9/2	−0.16	b.c.c.	10.9	.190[c]
Tl^{203}	29.52	2.433	16.12	1/2		h.c.p.	17.24	
Tl^{205}	70.48	2.457	16.28	1/2		h.c.p.	17.24	~ .006[b]
V^{51}	~ 100	1.1193	7.42	7/2	0.2	b.c.c.	8.5	.788 ± .008[d]
Pt^{195}	33.7	0.9153	6.06	1/2		f.c.c.	9.10	.030[e]
He^3 solid		3.243	21.5	1/2		b.c.c.	24	

[a] A.G. Anderson and A.G. Redfield, *Phys. Rev.* **116**, 583 (1959).

[b] $T_1 T$ for In and Tl was estimated by the Korringa relation from the Knight shifts for In given by D.R. Torgeson and R.C. Barnes, *Phys. Rev. Letters* **9**, 225 (1962), and for Tl given by N. Bloembergen and T.J. Rowland, *Phys. Rev.* **97**, 1679 (1955).

[c] K. Asayama and J. Itch, *J. Phys. Soc. Japan* **17**, 1065 (1962).

[d] J. Butterworth, *Phys. Rev. Letters* **5**, 305 (1960).

[e] R.E. Walstedt, E.L. Hahn, C. Froidevaux and E. Geissler, *Proc. Roy. Soc.* (London) A284, 499 (1965).

$C_L \gg C_S$, T_S will approach T_L with the time constant $R_{SL} C_S = T_1$. Writing $C_S = b/T^2$, where b is a parameter independent of temperature, one finds

$$R_{SL} = (\beta/b) T. \tag{5}$$

Examination of equation (3) for the spin entropy of the metal shows that

$$b = \frac{4}{3} V \frac{RT^2}{v} x^2 I(I + 1), \tag{6}$$

where V is the volume of metal, v is the molar volume, and R is the gas constant. Applying the definitions of thermal resistance and the conservation of energy, one finds the equations

$$\frac{d}{dt} (T_S - T_3) = -\frac{1}{R_{SL} C_S} (T_S - T_L) - \frac{1}{R_{L3} C_3} (T_L - T_3) \tag{7}$$

TABLE 2

Entropy removal per unit volume in a field of 30,000 gauss at 15 m°K.
The quantity $x = g\beta H/2kT$.

Substance	$x^a/$	$-\Delta S/nR$	$-\Delta S/V$ $(10^5$ erg/cm^3°K$)$
Aluminum	.0532	.01652	1.379
Copper	.0554	.00767	.895
Indium	.0448	.0332	1.758
Niobium	.0500	.0412	3.15
Thallium	.1176	.00691	0.333
Vanadium	.0537	.0303	2.96
Platinum	.0255	.000325	.0297
Solid He^3(24 cm^3/mol)	.1556	.01212	.420

[a] An effective x is given for Cu, In, Tl, and Pt which takes account
of the relative abundance of each contributing isotope.

and

$$C_L \dot{T}_L = - (C_S \dot{T}_S + C_3 \dot{T}_3). \tag{8}$$

For the present application, these equations may be very substantially simplified. In the first place, one has $C_L \ll C_3$. For example, in the case of copper [27] $C_L = 0.98 \times 10^3 \, TV_L$ erg/cm^3°K^2, $C_S = 4.5 \times 10^{-8} \, V_L H^2 T^{-2}$ erg °K/cm^3 gauss^2, while $C_3 = 7 \times 10^6 \, TV_3$ erg/cm^3°K^2. Hence $C_L/C_S = 2.2 \times 10^{10} T^3 H^{-2}$ gauss^2/°K^3. At 10 m°K $C_L/C_S = 1$ when $H = 148$ gauss. Since actual fields will be much larger than this value, one can assume that C_L is negligible compared both with C_S and C_3. In this case there will be a single time constant, T_b, which is

$$T_b = (R_{SL} + R_{L3}) \frac{C_S C_3}{C_S + C_3}. \tag{9}$$

It is instructive to calculate the ratio R_{SL}/R_{L3}. If it is assumed that $R_{L3} = \Gamma/T^3$, one finds $R_{SL}/R_{L3} = \beta T^4/b\Gamma$. Γ may be estimated from a value given in Anderson, Connolly, and Wheatley [6] for insulated copper wires, so that one finds $R_{SL}/R_{L3} = 1.5 \times 10^{13} T^4 d^{-1} H^{-2}$ cm gauss^2/°K^4, where d is the diameter of the wire and where it is assumed that all of the outside surface of the wires is in contact with the He^3. Taking again $d = 1.3 \times 10^{-3}$ cm and $H = 2 \times 10^4$ gauss at a temperature of 10 m°K one finds $R_{SL}/R_{L3} = 0.3$. This calculation shows that the thermal resistance between the nuclear spin and the lattice may be an important consideration in nuclear cooling. It is difficult to guess how the value of R_{SL}/R_{L3} will vary on adiabatic demagnetization since the magnetic field will always drop much more rapidly than T due to irreversibility and due to the presence of the He^3.

It would also be interesting to use the nuclear magnetism of the metal as a thermometer for

the temperature of the He^3. The above time constant considerations show that at temperatures of the order of 1 m°K, the equilibrium time between the thermometer and the He^3 would be rather long. Even if the Kapitza resistance could be neglected the thermal time constant for copper would be over a thousand seconds at 1 m°K under the reasonable assumption that $C_3 \gtrsim C_S$. In this connection we note that in the case of platinum the thermal time constant at 1 m°K would be expected to be of the order of 30 sec, which is much more reasonable.
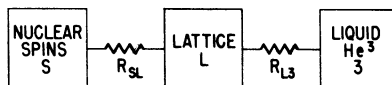
FIGURE 1

Thermal reservoirs and resistances for the cooling of
liquid He^3 by a paramagnetic.

The best known electron paramagnetic for the present purposes is cerium magnesium nitrate (CMN). CMN has many diamagnetic atoms for each cerium ion so that the distance between cerium ions is large and their interaction correspondingly weak. The cerium ion has no hyperfine structure, and its ground state is a Kramer's doublet with an effective spin of one-half. The magnetic heat capacity in zero external field is determined almost entirely by dipole-dipole interaction between the ions. The substance obeys Curie's law to below 10 m°K. It is highly anisotropic magnetically having $g_\perp$ = 1.84 [28] and $g_\parallel$ < 0.03 [29]. The very low temperature properties are not well determined. The original work of Daniels and Robinson [30] suggested that a lower limit of 3 m°K could be obtained with this salt. Their data were subsequently reanalyzed by de Klerk [31] who found that temperatures below 2 m°K were obtained. Subsequent experiments by Hudson, Kaeser, and Radford [32] suggested that even lower temperatures still were obtained for the same entropy. Daniels and Robinson also determined the relationship between the magnetic temperature and the Kelvin temperature for a single crystal ellipsoid of CMN. If their results are reduced to a spherical shape it is not obvious that they would predict the very low temperature magnetic properties of a powder of the same shape, the CMN being highly anisotropic. Hence it may be desirable to use a right circular cylinder of powder with diameter equal to height rather than a sphere, since it is then possible to obtain a more uniform loose packing of the powder.

All of the above workers are in agreement that the final temperatures possible with CMN are at least as low as 3 m°K. This is certainly a very large step downward from all previous work and hence CMN merits serious consideration. Although many paramagnetic crystals suitable for low temperature research suffer chemical changes on powdering, principally loss of water, CMN apparently does not. The crystals may be powdered to sizes less than 10^{-2} cm without deleterious effects. Hence the Kapitza resistance to these crystals may be lowered substantially. Using the same Kapitza resistance between the CMN and He^3 as has been measured between expoxy walls and He^3 and using a typical packing in which 60 per cent of the volume of the cell contains CMN and 40 per cent contains He^3, one predicts a thermal time constant of approximately 1000 sec at a temperature of 5 m°K if the powder grains are spheres of diameter 10^{-2} cm.

The entropy of a powder of CMN vs H/T has been calculated with the assumption that $g_\parallel$ = 0 and is plotted in Fig. 2. The calculation is made assuming that there is a uniform distribution of the crystallographic axes of the grains over a sphere, so that one has

$$\frac{<S>}{nR} = \int_0^{\pi/2} [\ln 2 + \ln \cosh x - x \tanh x] \sin \theta \, d\theta, \tag{10}$$

where $x = (g_\perp \sin \theta) \beta H / 2kT$, β is the Bohr magneton, and θ is the angle between the crystal axis and the magnetic field. For low values of H/T the curve corresponds to an isotropic paramagnetic with $g = 1.84 \sqrt{(2/3)}$ For large values of H/T the entropy is considerably more than that estimated assuming this g. One can see from the graph that most of the entropy is removed from the CMN powder when H/T is approximately 100,000 gauss/°K. This value of H/T is achieved at 15 m°K in a field of 1500 gauss. From a technical point of view it is desirable to use as large a field as possible on the CMN in order that the heat of magnetization of the CMN be transferred at a higher temperature, the corresponding entropy increase of the preceding refrigeration stage thus being as small as possible. Such a field is very easily arranged by means of a small superconducting solenoid.
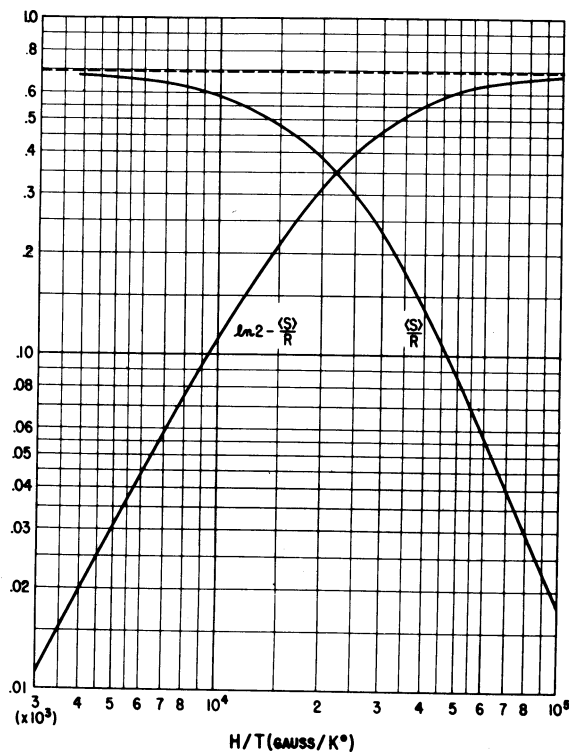

FIGURE 2.

Spin entropy and spin entropy removed for a powder of cerium magnesium nitrate in an external field H at temperature T.

For $H/T = 10^5$ gauss/°K the entropy removed per ion is approximately 0.68 k, where k is Boltzmann's constant. The corresponding numerical value for the entropy change of CMN is, per unit volume of CMN powder, $\Delta s = -1.5 \times 10^5$ ergs/cm³°K. For comparison the entropy per unit volume of liquid He³ at 15 m°K is 1.05 x 10^5 ergs/cm³°K. Hence substantial cooling should be expected from an initial temperature of 15 m°K for approximately equal volumes of CMN powder and He³ mixed together.

In the case of cooling by adiabatic demagnetization of CMN the lattice heat capacity, C_L in

Fig. 1, may always be assumed small. There results a single spin-bath relaxation time given by equation (9). Both the thermal resistance, R_{SL}, and the spin-bath relaxation time, T_b, in magnetically diluted CMN and in several other magnetic crystals have received considerable attention recently. In the case of crystals of lanthanum magnesium nitrate containing 2 per cent and 0.2 per cent of cerium, Ruby et al. [33], with some results quoted in Scott and Jeffries [34], found that T_b was limited by the so-called "phonon bottleneck" [35]. In these crystals the "direct" process, in which a single phonon is emitted or absorbed, is responsible for the spin-lattice heat contact at low temperatures. For cerium ions the direct process is sufficiently effective that the principal thermal resistance is that between the phonons in contact with the spins and either the rest of the phonons or the bath. Recently Miedema and Mess [36] have made simple thermal resistance measurements of R_{SL} in the case of $CuCs_2(SO_4)_2 6H_2O$. Both Miedema's R_{SL} measurements and Jeffries's T_b measurement on diluted CMN may be described by the heat flow formula

$$\frac{T'_S - T'_L}{\dot{Q}} = \frac{1}{kV} \frac{2\pi^2 v_0{}^3}{3 \ \omega^2 \ \Delta\omega} \ t_{ph},\qquad(11)$$

where k is Boltzmann's constant, V is the crystal volume, v_0 is an average velocity of sound, ω is the angular frequency of the center of the spin resonance line of width $\Delta\omega (\hbar\omega = g\beta H_{ext})$, t_{ph} is a phenomenological mean free time for scattering of a phonon out of the frequency band $\Delta\omega$ due to interaction with the bath, imperfections, or with other phonons, $\dot{Q}$ is the heat flow rate, and

$$T' = \frac{\hbar\omega}{k} \ / \left[\exp\left(\frac{\hbar\omega}{kT}\right) - 1 \right].$$

This formula follows if one assumes that the heat flow in time dt is just dt/t_{ph} times the difference in energy between the oscillators in equilibrium with the spins at temperature T_S and those in equilibrium with the lattice at temperature T_L. In the work of Miedema and Mess the quantity t_{ph} was found by independent experiments to be independent of temperature, magnetic field, and bath contact area. It was equal approximately to the time required for a phonon to cross the crystal ten times. Hence the phonons were probably relaxing to the phonon bath of the crystal itself via the crystal surfaces. But in the case of Ruby et al., t_{ph} was given approximately by the time for a phonon to move about half the crystal thickness, and in this case it may be that the phonons are in best contact not with the phonons of the crystal, but rather with the surroundings of the crystal. This possibility, seemingly in contradiction with the typical assumptions upon which theories of the Kapitza resistance are based [69], is given some substance by the calculations of Mills [37], who finds that, if the crystal surface is porous and in contact with liquid helium, the reflection coefficient for phonons coming from within the crystal is essentially zero.

If, in the case of CMN, the thermal resistance between the spins and the He^3 bath were given by equation (11), then a low thermal resistance should be expected by finely powdering the CMN, as is actually done in the present experiments. In this connection we refer to the results of Nash [38], who found a relaxation time linearly decreasing with crystal size, for sufficiently small sizes, down to 37 microns or perhaps less. One can estimate a lower limit for the spin-bath thermal resistance under the conditions of very low temperatures and zero external fields, where $\hbar\Delta\omega \gtrsim kT$. Assuming that all phonons are available for relaxing the spins, and that this process is very effective, and moreover assuming that the phonons exchange energy with the He^3 bath in a time t_{ph} approximately equal to the time required to cross half the crystal, one finds from equation (11) that the total thermal resistance is, for $\Delta T \ll T$,

$$R = \frac{\Delta T}{Q} = \frac{1}{kV} \frac{5}{2\pi^2} \left(\frac{\hbar v_0}{kT}\right)^3 t_{ph} . \tag{12}$$

If one assumes that $V = 1$ cm³, $v_0 = 2.5 \times 10^5$ cm/sec, and that the relevant heat capacity in the thermal relaxation time formula, equation (9), is that of 1 cm³ of He³, $7 \times 10^6 T$ erg/°K², then one finds $T_b \approx 8 \times 10^4 t_{ph} T^{-2}$°K². For a half thickness of 100 μ, as is typical in the experiments presented here, $t_{ph} = 4 \times 10^{-8}$ sec, so that at 5 m°K one has $T_b \approx 130$ sec.

It appears from the above that CMN *may* have a surprisingly low spin-bath thermal resistance when immersed in liquid helium. Taking $t_{ph} = L/2v_0$, where L is a typical crystal size, this resistance will vary inversely as the surface area, so very fine powdering of the CMN will substantially lower the resistance. It would be very interesting to perform experiments similar to those of Miedema and Mess, except with the CMN in a liquid helium bath, to study this point.

Comparing the nuclear and electronic paramagnetic cooling methods, then, we find that for reaching a temperature region above 1 to 2 m°K the potentiality of both is about the same. For lower temperatures one might consider finer and finer powders of electron paramagnetic material, but in the case of nuclear demagnetization there is a fundamental limit to this method imposed by the thermal resistance between the spins and the lattice. Since much smaller fields are needed for electronic cooling, compared with the nuclear cooling, the former is considerably easier to effect than the latter and hence has formed the basis for our technique of producing He³ temperatures in the millidegree range.

III. EXPERIMENTAL APPARATUS AND METHOD

A. Helium Cryostat

In all previous work in this laboratory the vacuum jacket surrounding the demagnetization apparatus and the He³ refrigerator was immersed directly in the main liquid helium bath, which was pumped to approximately 1.2°K following transfer. Magnetic fields were provided by means of an iron magnet. This simple apparatus had several disadvantages which prevented us from obtaining extremely low temperatures. One of these was the relatively small amount of working space available (2.77 cm diam by 45 cm long). Another disadvantage was that at extremely low temperatures it was very difficult to do resistance thermometry since the apparatus could not be shielded from radio-frequency fields. The resistance thermometry is useful not only in actual measurements but also as an indication of how the demagnetization process is proceeding. The radio-frequency interference also was capable of heating the samples. Moreover, the use of an iron magnet was disadvantageous because it was not possible to magnetize and demagnetize various parts of the experimental apparatus simultaneously. Perhaps the most serious disadvantage was that the main helium bath had to be refilled approximately every 12 hr, and this refilling process always resulted in a partial warming of the sample. In the present cryostat these disadvantages have been overcome. The working space is 4.3 cm diam x 65 cm long and is located inside a vacuum jacket of outside diameter 5.0 cm. The cryostat and associated measuring equipment are located inside a shielded room which provides over 80 db of attenuation for frequencies of order 100 Mc/sec. We have had no problems with radio-frequency heating in this room. The main bath of the cryostat is maintained at atmospheric pressure except during calibration of the magnetic thermometer. Within the vacuum jacket is a He⁴ evaporator consisting of a copper pot of approximately 60 cm³ volume which serves both to cool a thermal shield placed in the

vacuum around the demagnetization apparatus and to condense He^3 for the He^3 refrigerator. By means of a small valve located in the main He^4 bath the He^4 evaporator may be filled in one or two minutes without ever raising its temperature above the lambda point. The evaporator is pumped through a 1 mm diam orifice using an NRC type B2 booster diffusion pump in series with a Welch type 1402 mechanical pump. Temperatures of the order of 0.8 to 0.9°K are obtained. The evaporator must be refilled about once every 24 hr. Transferring helium and nitrogen into the main dewars has no effect on the temperature of the sample.

He^3 for the He^3 refrigerating system is condensed in a rough-walled cylinder in contact with the He^4 evaporator. At the bottom of the condenser is a valve consisting of a brass seat with a 0.018 in. diam hole and a hardened beryllium copper needle. A 15 cm length of 1/64 in. o.d. x 0.003 in. wall cupronickel tubing leads to the ∼ 2 cm³ volume He^3 evaporator, which is pumped by means of an NRC type B2 booster pump in series with a Welch type 1402 KBG pump modified for He^3 service. This evaporator maintains a temperature of about 0.27°K after demagnetization of the apparatus suspended from it.

In the present experiments a thermal shield at 0.3°K has not been used in order to allow more space for paramagnetic salts. The apparatus works satisfactorily under these conditions, but perhaps the heat leak might have been improved if a shield at 0.3°K had been used.

Magnetic fields are provided by superconducting solenoids. One solenoid is 8 in. long, uniformly wound, and provides a field of 15,000 gauss at its center. This solenoid, constructed by the Westinghouse Electric Corporation [39], requires a current of 16.3 amp for rated maximum field. The second solenoid, built in this laboratory, is 4 in. long, 2.5 in. in diameter, and provides a field of 2600 gauss at its center with a current of 15 amp. Both solenoids are provided with persistent-current switches so that the field may be left on without external excitation. Current for the solenoids is supplied by a transistorized current supply [39] which is used alternately with the two solenoids by means of appropriate manipulation of the persistent-current switches. The current from the supply may be adjusted by means of an infinite resolution 10-turn potentiometer. Moreover, the current corresponding to the maximum dial reading of this control may be adjusted continuously from zero to rated maximum current using a second 10-turn potentiometer. It is very advantageous to increase current resolution at low currents. At one time the solenoids were powered by a transistorized supply in which a conventional 10-turn wire-wound control was used. The current jumps which resulted as the wiper on the control moved from wire to wire proved to be harmful sources of eddy-current heating. Each solenoid is supported from the top of the cryostat by means of two strands of braided nylon line [40]. The nylon line passes through a series of teflon guides and then is directed to a special enclosure on one side of the pumping head where there are two winches, one for each solenoid. The solenoids are usually positioned a bit lower than desired over the paramagnetic salts, since, when the heat of magnetization is carried away and the salts develop a magnetic moment, the strong magnetic forces generally raise the solenoids somewhat. The solenoids are also energized so that they repel one another, the extra stresses being taken up by the nylon lines. In the present arrangement, the magnetic temperature measuring coils are located near the bottom of the cryostat. For this reason, during calibrations and during the measuring period, the solenoids are raised as far as possible. The diamagnetism of the superconducting wire may cause very substantial zero shifts of the magnetic temperature scale if the solenoids are too close to the measuring coils. We have had no difficulties with remanent fields preventing the attainment of sufficiently low temperatures, although motion of the solenoids while they are being raised sometimes does give brief eddy-current heating. Flexible electrical leads to the solenoids are provided by means of ten strands of Formex insulated 0.010 in. diam copper magnet wire. Electrical connections to the solenoids are made readily disconnectible by disassembling BNC connectors and using the male and female contacts only. The female part is pushed into a

Bakelite ring permanently attached to the solenoid while the male part is soldered to the end of the flexible leads. Each solenoid has four such electrical joints, two for the main current leads and two for the heater leads of the persistent-current switch.

Thermal grounding is provided within the vacuum space of the cryostat for 36 separate electrical leads. Thermal grounding is made at the temperature both of the He^4 evaporator, 0.9°K, and of the He^3 evaporator, 0.3°K. The thermal grounding strips are made out of copper rings through which a number of holes, equal to the number of thermal grounds desired, have been drilled. The rings are about 1 in. high. Copper wires of 0.040 in. diam, insulated by # 26 glass spaghetti [41], are passed through these holes and the space between the wires and the copper ring is filled with Epibond 100A [42], a thermal setting epoxy resin.

B. General Demagnetization Apparatus

By general demagnetization apparatus is meant that part of the apparatus designed for temperatures below that of the He^3 refrigerator, including the main paramagnetic refrigerators and thermal insulation, but not including the apparatus associated with the experiment immediately at hand. The demagnetization apparatus is standard and used from one experiment to the next. The principal structural materials used are nylon, teflon, and Epibond 100A, thermal contact being made by coil-foil [43] used in a variety of ways. At the top of the demagnetization apparatus is a small cylindrical copper piece which slides over the bottom of the He^3 evaporator and is pinned in place. Screwed into this copper piece is a nylon rod, 8 mm in diameter and bored out to leave a 1 mm wall over a distance of 4 cm and so provide thermal isolation from the He^3 evaporator. A nylon distance piece whose length may be changed according to the experiment separates the nylon thermal insulator from the thermal guard and the main refrigerator. The thermal guard crystals are ferric ammonium alum and the main refrigerator crystals are chromium potassium alum. Both are mounted on nylon bases constructed as follows. Part of the center portion of a 34 mm diam nylon rod is removed symmetrically on opposite sides so as to leave a flat plate 34 mm in width, 3 mm thick, and sufficiently long to accomodate the alum crystals with due allowance for the greater thermal contraction of the nylon. The ends of the rod are left cylindrical to facilitate mechanical assembly. The upper cylindrical end of the nylon base supporting the thermal guard has a hole bored into it so that the nylon distance piece may be pinned into position. The lower cylindrical end of the base is threaded over a 5 mm length with a 3/4 in. - 16 NF thread, as is the upper end of the chrome alum base. The two bases are joined together by means of a teflon collar, 25 mm long x 3 mm wall threaded on the inside so that the two bases may be screwed tightly together and kept well aligned, although thermally isolated [44]. At the bottom of the main refrigerator base is left a cylindrical boss, 8 mm in diameter and 30 mm long, so that various experiments may be fastened to it.

Both the thermal guard crystals and the main refrigerator crystals are 3 mm thick slabs cut from larger single crystals using a water-cooled carborundum wheel. Thermal contact to these crystals is made using Apiezon N grease [45] and coil-foil following the technique described in Anderson, Salinger, and Wheatley [25]. The thermal guard is 8 cm long and contains 70 grams of iron alum. The main refrigerator is 10 cm long and contains 110 grams of chrome alum. In each case four layers of crystals are placed on each side of the nylon base. These are formed by two packages of two layers each having coil-foil on all sides. In the case of the main refrigerator crystals, the coil-foils used for cooling the He^3 cell (labelled B in Fig. 3) are placed between the nylon base and the inner package of crystals and between the two packages of crystals. A single coil-foil connects the two sides of the base. Both the He^3 filling tube and a heater of about 200 ohms resistance are thermally connected to this foil. After the crystal packages are assembled on the nylon bases, pieces of special coil-foil in which half the wires are glued

perpendicularly to the other half are wrapped around the crystal package, and securely bound with No. 40 cotton thread. Speer carbon resistors [46] prepared as indicated in Black, Roach, and Wheatley [47] are attached to both the thermal guard and the main refrigerator to monitor their temperatures. Thermal contact between the main refrigerator crystals and the thermal guard crystals is obtained by means of a lead thermal switch 5 mm wide, 20 mm long, and 0.2 mm thick. The switch is located between the two groups of crystals directly over the teflon collar. It is soldered to a coil-foil which had one end specially prepared as follows. The insulation was removed from the ends of the wires which were then clamped in a hairpin-shaped piece of 0.020 in. diam copper wire and dipped in hard solder. The resulting globule was then filed flat. This allowed a minimum of Pb-Sn solder to be used in attaching the lead switch. This switch is oriented so that the direction of the heat flow is parallel to the magnetic field. The thermal switch to the He^3 evaporator is of similar design and is located approximately 6 cm above the top of the thermal guard crystals in order that it be thermally conducting only when the main field is close to its maximum value. Calculations show the principal thermal impedance during magnetization is likely to be neither in the greased contact nor in the lead switches but instead in the copper coil-foils, so that about 1500, 0.002 in. diam insulated copper wires are connected to each switch. The quantities of thermal guard crystals and main refrigerator crystals were determined by the somewhat arbitrary requirement that the thermal guard should stay below 0.1°K for approximately three days on the basis of the calculated heat influx to that part of the apparatus. Then as much chromium alum was put in as possible, consistent with the overall length of the main solenoid. None of the experiments here suffered from a lack of these paramagnetic refrigerants.

We now consider a number of points of general interest. First, all of the structural materials contract at least 1 per cent in length on cooling. It is possible to develop substantial thermal stresses when two materials of different expansion coefficient are placed in mechanical contact. During the initial experiments the crystals were assembled on Epibond 100A bases, but it was found that sometimes these fractured due to thermal stresses caused by the crystal packages so that now nylon is used for this purpose, the nylon being stronger. Secondly, at one time rather large amounts of Pb-Sn solder were used in the construction of the apparatus, particularly in the assembly of resistance thermometers and in making thermal connections between different parts of the apparatus. During the demagnetization, at fields of several thousand gauss and below, it was found that when the field was changed the resistance thermometers indicated rather high temperatures, the effect becoming steadily more pronounced at lower fields. This heating effect became very much smaller on removing as much Pb-Sn solder as possible from the apparatus. The heating effect is not noticeable in such soft superconductors as lead or zinc. Third, the lower part of the vacuum jacket consists of a tube of Epibond 100A sealed onto the end of the metal as described by Wheatley [48]. It was difficult to make this section of the apparatus sufficiently light-tight to eliminate radiation heat leak. A solution to the problem was as follows. The Epibond 100A tube was painted with a fifty-fifty mixture by volume of "Dag" [49] and General Electric 7031 varnish [50] mixed with toluene in a one-to-one proportion. Although this paint can soften and damage the 100A if left in contact with it in the liquid state for a long period of time, there is no difficulty in its normal use where it quickly dries. In addition a coil-foil shield was made which just fit over the outside of the 100A vacuum jacket. This shield was made on a teflon form by laying down ordinary coil-foil parallel to the axis and then close-winding a single layer coil of 0.002 in. diam Formex insulated copper wire over it. To reduce further the radiation leaks this was painted with the mixture of "Dag" and 7031 varnish mentioned above, allowed to cure for an hour or so in an oven at 50°C, and then removed from the teflon form. The insulation is removed at the top of this shield and the wires placed in electrical contact with the metal portion of the vacuum jacket. The vacuum jacket is thus completely Faraday shielded. Fourth, the apparatus is centered inside the 0.9°K thermal shield by means of three tightly fitting pieces of cotton batting tied to the bottom of the thermal guard. The cotton was originally introduced as a soft support to avoid

vibration heating, but we cannot comment quantitatively on its success. At one time the whole demagnetization apparatus was supported at the top from a "soft" support consisting of six strands of nylon line [40]. The transition from this soft support to the more rigid one, described earlier in this section, did not give a marked change in the heat leak. In another experiment, in an attempt to improve the centering of the apparatus, a centering device was used which consisted of two nylon rings, the inner one in contact with the section immediately below the main refrigerator, the outer one in contact with the inside of the He^4 shield, and the two separated by twelve "spokes" of No. 40 cotton thread which had been threaded through the rings. This arrangement gave excellent centering and no observable conduction heat leak, but did contribute a substantial heat leak due to vibrations.

C. Apparatus for Heat Capacity Measurements

The heat capacity apparatus in its simplest form is shown in Fig. 3. The He^3 and CMN powder are located in a right circular cylindrical cavity with diameter equal to height, surrounded by a cylindrical block of Epibond 100A [42], in which copper wires (B) are imbedded for the purpose of precooling the contents of the cavity to a temperature of about 15 m°K. This apparatus was constructed as follows. The discussion may be more readily understood by referring to Fig.3. A cylindrical, precast piece of Epibond 100A was machined to the diameter desired for the cavity. Eight strips of coil-foil each 15 in. long by 1/2 in. wide and containing 400, 0.002 in. diam Formex insulated copper wires, were laid axially along the rod and held in place with cotton thread. In the region of the cavity the foils had not been coated with GE 7031 varnish. The Epibond rod was placed horizontally in a rotating device in an oven, and Epibond 100A was sprinkled over the non-varnished wires until they were thoroughly impregnated. The rod was then placed in a teflon mold and the mold filled with epoxy so as to produce the exterior form shown in Fig. 3.

After the epoxy had cured, the cavity was bored and a counter-bore was made to accept the epoxy plug (F). Five 0.020 in. diam radial holes were drilled into the cavity. A 1/64 in. o.d. x 0.003 in. wall cupronickel He^3 filling tube (C) was sealed into one of these holes with Epibond 100A. The other holes were next used to accommodate the leads from an electrical heater and a resistance thermometer, these leads being sealed in with Epibond 121 [42]. The heater (E) consisted of a 5 in. length of 0.002 in. diam Evanohm wire arranged in an approximate helix in the center of the cell. The heater leads were two 99.999 per cent pure, 0.004 in. diam copper wires, the four-wire connection being made outside the cell. The potential differences were measured using a Leads and Northrop type K-3 potentiometer.

The resistance thermometer (D) was made using a technique developed by J.I. Connolly. In this technique a standard half-watt type 1002 Speer carbon resistor is cut with a diamond saw into thin wafers about 0.010 in. thick, the outside shell of phenolic resin being left intact. Manganin or copper leads of 0.002 in. to 0.004 in. diam are then attached with silver paint [52]. After the paint is dry a very thin coat of Epibond 121 is applied for protection. This technique was adopted to provide a geometrically small resistor which presented a maximum surface area for dissipating the measuring power by means of the He^3 bath. These resistors continue to indicate down to about 10 m°K but probably not at very much lower temperatures. At the very lowest temperatures, those with copper leads tended to take on the temperature of the walls rather than the temperature of the helium. Manganin leads of 0.002 in. diam proved to be the most satisfactory. The resistances were measured using an a.c. Wheatstone bridge.

The CMN (A), powdered and having been recently passed through a standard NBS 40 sieve, was next loaded into the cell until the cell was completely full. A small glass rod was used to
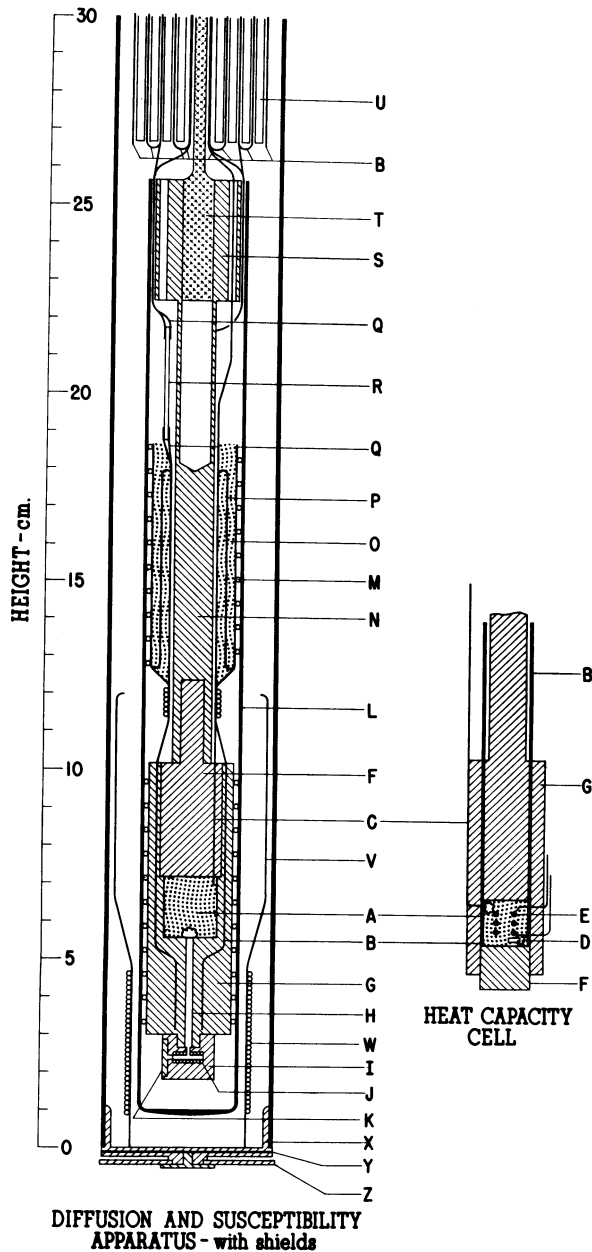
FIGURE 3

Drawing in correct relative proportion of the He³ sections of the apparatus used for thermal and magnetic measurements. (A) CMN powder; (B) copper wire sheath and coil-foil; (C) filling tube; (D) resistance thermometer; (E) heater; (F) main cell end plug; (G) main cell body; (H) interconnecting hole; (I) magnetic measuring cell body; (J) pickup coil; (K) measuring cell end plug; (L) thermal shield; (M) helical insulator of thread; (N) distance and insulating piece and mechanical support; (O) CMN-silicone oil slurry; (P) copper thermal contact wires; (Q) joint to zinc switch; (R) zinc switch; (S) upper support; (T) boss extending below main refrigerator; (U) 3 mm chrome alum slabs; (V) coil-foil Faraday shield; (W) pulse coil; (X) 0.9° thermal shield; (Y) end plug and thermal shield; and (Z) nylon spacer.

compress and distribute the CMN and thus to insure uniform packing. The powder always handled as though it were rather dry even though examination of it under a microscope never gave any indication of dehydration.

In this apparatus the thermal resistance between the He^3-CMN "calorimeter" and its surroundings is the Kapitza resistance. If the temperature of the chrome alum is in the region of 15 m°K or below, this resistance is sufficiently large to make specific heat measurements possible. However, it is difficult to obtain a heat capacity measurement at a temperature much higher than that of the chrome alum. In order to obtain heat capacity measurements at somewhat higher temperatures a thermal switch of zinc, about 1 cm wide, 2 cm long, and 0.2 mm thick, is interposed between the chrome alum and the heat capacity cell. The ends of the copper wires from both the chrome alum and the heat capacity cell are dipped in hard solder and filed flat as described above, and then pre-coated with zinc. The zinc switch is melted directly onto the ends of these wires thus avoiding all use of soft solder. Zinc is used because of its very low critical field, which allows the heat capacity cell and the chrome alum refrigerator to be thermally connected except at very low fields. Measurements were made on two different heat capacity cells. In the first the CMN mass was 1.491 g and the diameter of the cell, which equaled its height, was 1.207 cm. In the second cell the mass of the CMN was 1.546 g and the diameter and height were equal to 1.220 cm. In the second cell a zinc thermal switch was used while in the first cell the foils around the cell were connected directly to the chrome alum.

The number of moles of He^3 in the cell was determined in a separate cryostat in which a short tube was connected to the cell and the amount of He^3, condensed at 1.3°K, was measured by means of a Toepler pump of calibrated volume in conjunction with a constant volume manometer. The result was corrected for the amount of He^3 in the filling tube, for the change of density between 1.3°K and 0°K, and for any effect of pressure. Several determinations of the number of moles of He^3 in the cell agreed to better than 1 per cent.

The mutual inductance for measuring the magnetic susceptibility of the CMN consists of two identical sets of primary and secondary coils. These were wound side by side on a 0.003 in. thick mylar sheet wrapped around a split mandrel of 2 in. o.d. The primaries are each 1.60 in. long with a center separation of 2.4 in. Each secondary, 1.40 in. long, was wound directly over its primary with an intervening mylar sheet. Each primary contains 539 turns, and each secondary 2128 turns, of 0.0031 in. diam, heavy Formex insulated copper wire wound at 85 turns/in. The coil set which is not to be centered over the CMN has an additional 55 turns in the secondary, these being tapped every 11 turns. Each tap corresponds to a change in mutual inductance which is a little less than the range of the mutual inductance bridge. In this way it is possible to have reasonable sensitivity during calibration above 1°K and yet allow measurement of very low temperatures.

The bridge is a Cryotronics [53] 17 c/s electronic mutual inductance bridge. The general use of this instrument, and the technique of using small quantities of CMN, have been discussed in the paper by Abel, Anderson, and Wheatley [54]. There it is shown that the 17 c/s susceptibility of CMN is the same as that measured ballistically down to 15 m°K, within an accuracy of 0.1 per cent. During the course of the present work, it was found that these two susceptibilities are equal, to within 0.1 per cent, down to 4 m°K, the lowest temperature at which a comparison was made.

D. Apparatus for Nuclear Magnetic Measurements

1. Sample cell

The apparatus for nuclear magnetic measurements by the spin-echo method is necessarily more

complicated than that required for specific heat measurements since the measurements themselves are more complex. The general techniques are rather similar to those described by Anderson, Reese, and Wheatley [21]. The aim of the measurements is to measure the nuclear magnetic susceptibility, χ, and the self-diffusion coefficient for the magnetization, D. Using the same apparatus and practically the same arrangement, it is possible also to measure the spin-lattice relaxation time, T_1, for the He^3. In order to make these measurements, four coils are needed. One produces a homogeneous steady precession field, H_0. The second produces a homogeneous field gradient, G, parallel to H_0. A third produces a linearly polarized pulse field, $2 H_1$, perpendicular to H_0. The fourth is a pickup coil with axis perpendicular both to H_0 and $2 H_1$, to detect the precession of the nuclei in the field H_0. Only measurements of D require the externally controlled gradient G.

The external magnetic field H_0 is nearly uniform over all the region containing the He^3 and the CMN used to cool it. Therefore the CMN is magnetized and acts approximately as a magnetic dipole. Thus it is necessary to remove the region of He^3 in which magnetic measurements are made to a distance sufficiently far from the CMN that the residual field gradient resulting from this dipole is small. The residual gradient is linearly proportional to H_0 and depends on the geometry. The gradient G required to measure D depends on the magnitude of D and not on H_0. Hence low values of H_0 are desirable in order to reduce the residual gradient.

Another and a very important reason for keeping H_0 low is to avoid increasing the temperature of the CMN by adiabatic magnetization. An estimate of the effect of H_0 on the temperature may be made by considering the CMN only. The effect will be less in the presence of He^3. Temperature changes on adiabatic changes in field may be obtained from the equation

$$S/nR = \ln 2 - 1/2\, x^2 - b/T^2, \tag{13}$$

where

$$x^2 = \frac{2}{3} \left(\frac{g\beta H}{2kT} \right)^2 \ll 1,$$

and [31]

$$b = 3 \times 10^{-6}{}^\circ\text{K}^2 \ll T^2.$$

Using the relation that

$$S(0,\ T_0) = S(H,\ T_H) \tag{14}$$

one finds

$$T_H = T_0 [1 + (H/48.5\ \text{gauss})^2]^{1/2}. \tag{15}$$

The resonance frequency selected for this experiment was 60.0 kc/sec, corresponding to a resonance field H_0 of 18.5 gauss. Under these conditions $T_h = 1.07\, T_0$. Taking the He^3 into account makes the coefficient of T_0 closer to 1.

As mentioned above the separation between the He^3 upon which spin measurements are to be made and the CMN which cools it is determined at least in part by the residual gradient produced at the site of the measurement by the magnetism induced in the CMN by the applied field H_0. Both the measuring site and the CMN site are located on the cryostat axis and H_0 is taken to be perpendicular to the axis of the cryostat. For H_0 parallel to the cryostat axis the residual gradient aprallel to H_0 is an order of magnitude greater for the same separation between measurement site and CMN site. For reasons to be described later, the measurement volume

is taken to be a rectangular parallelepiped with two sides equal and much larger than the third, the third being parallel to the axis of the cryostat. The only field gradient which will have a large effect is that parallel to H_0. Setting up a coordinate system with z parallel to H_0 and origin in the center of the measurement volume, one finds for the residual gradient

$$\frac{1}{H_0} \frac{\partial H_z}{\partial z} \lesssim \frac{9z}{L^5} \left(\frac{\mu_{CMN}}{H_0} \right),$$
(16)

where L is the distance from the center of the CMN to the center of the measurement cell. At 4 m°K, $\mu_{CMN}/H_0 = 0.28$ cm^3 in the present cell. Also because of the magnetic moment of the CMN, the field at the center of the cell will be different from H_0 by the amount

$$\Delta H_0 = - \mu_{CMN}/L^3.$$
(17)

The maximum value of z according to other considerations is about 0.4 cm, so that with $L = 5$ cm and $T = 4$ m°K the maximum residual gradient due to the CMN is about 0.01 gauss/cm and the steady field H_0 is less than its value at high temperature by about 0.2 per cent.

The value of G must be large compared to the residual gradient but not so large that it results in excessive attenuation of the spin echoes. Expecting a low temperature of approximately 4 m°K and using the previously measured value [21] for the diffusion coefficient of 1.5 x $10^{-6}T^{-2}$ cm^2°K^2/sec, one finds that the maximum expected diffusion coefficient is approximately 0.1 cm^2/sec. Spin echoes are attenuated according to the equation [55]

$$\frac{h_2}{h_1} = \exp\left[-\frac{\gamma^2 G^2 D}{12} (t_2 - t_1)^3 \right],$$
(18)

where h_2 and h_1 are the amplitudes of two successive echoes, γ is 2.04 x 10^4 gauss^{-1} sec^{-1} for He^3, G is the field gradient, and $(t_2 - t_1)$ is the time interval between echoes. The recovery time of the electronics following a pulse is several milliseconds. The widths of the echoes, as mentioned below, are approximately 4 msec. Time must be allowed for the full diffusion pulse train, which consists of a 90° pulse followed at a fixed and relatively short time by a 180° pulse followed at a variable time by a second 180° pulse. Hence on the basis of recovery time and echo width, it is desirable that the echoes should not attenuate to less than 10 per cent of their original size in less than about 25 msec at the lowest temperature. This leads to a valuable of G of about 0.2 gauss/cm. This is over ten times larger than that expected from the residual gradient and is satisfactory.

The quantity G is also important in determining the echo width. For the case in which the cross-sectional area of the He^3 cell perpendicular to the gradient and to H_0 is independent of distance, the echo amplitude is proportional to the factor

$$\frac{\sin(\gamma G a t)}{(\gamma G a t)},$$

where a is the half-length of the cell in the direction of H_0 and G. The quantity a is determined by the requirement that, to avoid wall-effect problems, one should have $\sqrt{(2Dt)} \ll a$. Taking $t = 25$ msec and $D = 0.1$ cm^2/sec, one finds that a should be much greater than 0.07 cm. The half-length a was made equal to 4 mm in the present cell, corresponding to about a 3.8 msec time interval between the first zeros on each side of the maximum of the echo for a G of 0.2 gauss/cm.

Previous measurements [21] of the magnetic properties of He^3 were made with a cell having an inside diameter of 0.25 cm, a length of 2 cm, and a pickup coil of about 3000 turns with axis

parallel to the cylinder axis. Measurements were made in a field H_0 of 26 gauss. The signal was enhanced by a factor of 4 by means of a separate coil producing a field of about 100 gauss which was turned off shortly before the diffusion or susceptibility measurement was to be made. Such an enhancing field is not possible in the present experiment since it would increase the CMN temperature excessively. In the present experiment the quantity of He^3 must be kept small so that it can be cooled sufficiently. Hence the signal-to-noise ratio is expected to be less in the present experiment than in previous ones. However, a relative improvement was made through careful design, and tuning, of the pickup coil.

The cell dimension parallel to H_0 must be large enough to avoid wall effects, while the dimension parallel to the pickup coil axis, which is oriented perpendicularly to H_0 in order to pick up the precession signal, should also be long so as to provide good coil geometry. The third dimension which was taken parallel to the cryostat axis should be chosen small to limit the volume of He^3 which has to be cooled. Here the assumption is made that He^3 hitting walls which are parallel to H_0 will result in no wall effect on the diffusion along H_0. Thus a rectangular parallelepiped, 8 mm x 8 mm x 1.2 mm, was chosen as the measuring volume. Another possibility would have been to orient the pickup coil axis parallel to the cryostat axis, but in this case orientation of the 8 mm x 8 mm faces so as to be parallel to H_0 is much more difficult. The form of the cavity in its surroundings is shown in Fig. 4, which shows correctly
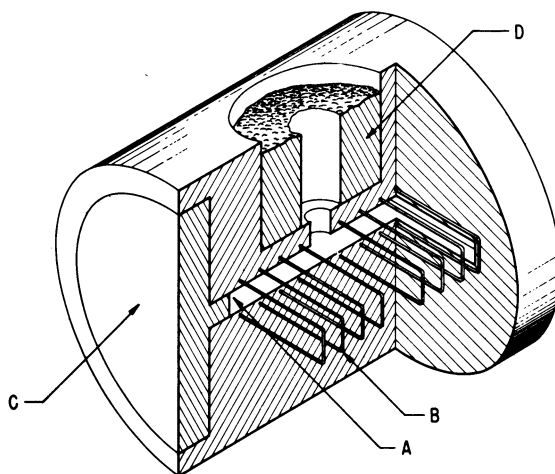

FIGURE 4

Cutaway view of magnetic measuring cell drawn in correct relative proportion.
(A) He^3 space; (B) pickup coil (schematic); (C) end plug; (D) bottom
extension of main cell body showing interconnecting hole.

the relative dimensions. One sees that the filling factor of the coil is excellent. The pickup coil (B) consists of 3100 turns of 0.0005 in. diam Solvar insulated copper wire [56]. To reduce distributed capacity, the coil is wound in 1/2 mm wide pi's of about 225 turns each. The center section is more complicated because of the entrance port. At a frequency of 65 kc/sec, and at helium temperature, the self-inductance of this coil is 29 mh; the distributed capacity is 23 pf; and the Q is 75. The natural frequency is about 200 kc/sec and the resistance 157 ohms. One Evanohm lead, 28 in. long by 0.002 in. diam, and one manganin lead, 28 in. long by 0.003 in. diam, are included in the circuit such that the total circuit resistance in the actual experiment and at low temperature, is about 800 ohms, the resulting Q being about 15. This gives

a very reasonable reproduction of the echoes.

The actual mechanical construction of the measurement cell, shown in Fig. 4, will be described in some detail since the method with variations is quite generally applicable. The object is to produce a cavity (A), 8 mm x 8 mm x 1.2 mm, with a centrally located port for admission of He^3. In addition, it is desired to wind on the cavity the 3000 turn coil described above with the best possible filling factor. The 0.0005 in. diam wire is extremely fragile, and hence this must be considered in the design. The construction material is Epibond 100A. First, a teflon mold is constructed from a 12.5 mm o.d. cylindrical rod. On one end of the rod is machined, in a symmetrical manner, a tongue 8 mm wide, 1.2 mm high, and 10 mm long. A 1 mm wide circular ledge of diameter 8.5 mm is then turned on the end of the circular rod adjacent to the tongue to provide eventually for a seat for the plug, part (C) in Fig. 4, which will enter 2 mm into the final cavity. This teflon mold is rotated in an oven while the tongue is covered with Epibond 100A, which is allowed to cure. It is then removed from the oven and the four sides of the rectangular part are machined so as to leave a 100A layer of thickness 1/2 mm around the teflon tongue, but with a raised portion of dimensions 6 mm high by 9 mm wide by 1 mm thick left on the side nearest (C). A length of 8 mm of teflon covered with Epibond 100A projects out beyond the raised portion. On a diameter of about 10 mm two 0.018 in. diam axial holes are drilled to accommodate two 0.005 in. diam copper leads, which are to be soldered just over the raised portion to the 0.0005 in. diam copper wire from which the coil is made. In the center of one 8 x 8 mm cavity face a hole of diameter 1.5 mm is bored through the 100A only. In it is sealed a tube of Epibond 100A, 1 mm i.d. and 1 mm high, using Epibond 121. After the 121 has cured a teflon cap, 1 mm in diameter and 3 mm high with a rounded top of about 1 mm radius, is inserted into this hole to facilitate the winding process. The form is now ready for the coil to be wound. The 0.0005 in. wire is soft-soldered to one 0.005 in. copper lead using a very small amount of solder. Then, in case the start of the wire might break, it is wrapped several times over the raised portion previously described, and the winding process begins. After the coil is wound, the final end is soldered to the other 0.005 in. wire. The teflon cap is removed from the central hole and replaced by a 6 mm diam teflon cylinder appropriately reduced at one end to fit into the 1 mm hole. This teflon plug projects just to the outside diameter of the final cell. A drop of Epibond 121 is placed on each exit hole for the 0.005 in. leads and allowed to cure. The whole assembly is inserted into a teflon mold, 12.5 mm i.d., which is then filled with 100A. After the cell has been cured it is removed from the mold and the teflon plug sealed into its side is removed by threading it and pulling it out. The side port is then counter-bored to a precise diameter so as to fit over the bottom of (G), Fig. 3.

The remainder of the He^3 apparatus is designed and constructed in the following way. The diameter of the tube (H), which communicates from the CMN volume (A) to the measuring volume must be as large as possible in order to reduce the thermal resistance between them. On the other hand, it must be as small as possible in order both to have a minimum He^3 dead volume and to reduce the heat input from the outside through the Kapitza thermal boundary resistance. A diameter of 2.2 mm is satisfactory. Assuming that the connecting tube is 4 cm long, the thermal time constant of the measuring volume with respect to the CMN volume is given approximately by $\tau = 3T^2 \sec/(m°K)^2$. The ratio of the thermal resistance of the He^3 column to the Kapitza resistance, R_W, of the walls may be estimated using the value of the Kapitza resistance given in Anderson, Connolly, and Wheatley [6] for an epoxy wall. This value is $R_W A T^3 = 3 \times 10^{-6}$ sec cm^2°K^4/erg, where A is the surface area. The resistance R_C of the He^3 column is approximately 2.1 T sec/erg, while that due to the wall is approximately $10^{-6} T^{-3}$ sec °K^4/erg. Hence one has

$$R_C/R_W = 2 \times 10^6 T^4 °K^{-4}.$$

At a temperature of 10 m°K the thermal resistance of the column is about 2 per cent of the wall

resistance. It may therefore be assumed that at 10 m°K and below all of the He^3 measuring volume, CMN volume, and communicating tube will have the same temperature, while the walls may be at an entirely different temperature.

We note in passing that this design forms the basis of a method for measuring the thermal conductivity of He^3 at very low temperature. The measurements by Anderson, Salinger, and Wheatley [18] of the thermal conductivity of He^3 could not be continued successfully below 30 m°K in the conventional type of thermal conductivity cell which was used, since the Kapitza thermal boundary resistance of ends of the cell became large compared with the thermal resistance of the He^3 itself. In an apparatus consisting of two larger volumes of He^3, separated by a narrow tube, the thermal resistance of the He^3 in the tube may be measured without introducing a boundary resistance in series with the bath. Hence this geometry should be appropriate for very low temperature measurements.

In the experiments on heat capacity, the ratio of He^3 volume to CMN mass is 0.44 cm^3/g. In the present cell it is desired to decrease this ratio somewhat. The volume containing the CMN is a right circular cylinder with diameter and height both equal to 15.6 mm. The CMN is packed more tightly in this volume than in the specific heat cell, the resulting ratio of total He^3 volume to CMN mass being 0.28 cm^3/g. In the D and χ measurements, one is not in principle as concerned as in the heat capacity measurement that the whole CMN − He^3 mixture be at a uniform temperature. It was hoped to reach a lower final temperature by using a tighter packing of the CMN.

The mechanical construction of the part (G) containing the CMN and the interconnecting tube is similar to that for the heat capacity cell. A piece of cured 100A is machined to dimensions approximating those shown in Fig. 3 for the space inside the coil-foil (B). A brass rod, smaller in diameter than the final cavity desired for the CMN, is inserted in the upper end to aid in centering the piece for final machining. At the opposite end, which at the start is oversize in length, is inserted a smaller brass pin also used to assist in subsequent centering. Apart from the holes made for the rod and pin, the 100A rod is solid, being 7 mm in diameter near the bottom as shown. The brass rod is covered with a tube of teflon with an o.d. somewhat greater than that of the plug (F) which is to be used to seal the cell. The outside of the assembly is next covered uniformly with 3600, 0.002 in. diam, heavy Formex insulated copper wires laid parallel to the axis of the rod and held tightly in place with cotton thread. The first 1200 wires are gathered together at one end and hard-soldered into a flat sheet as discussed previously. This is soldered later to the lower end (Q) of the Zn thermal switch. The other copper wires are left about 30 cm long and are used to make contact to the thermal guard (O). A thin sheet of teflon is wrapped over the wires where they pass over the teflon tube. The assembly is then placed horizontally in a rotating device in an oven and the exposed wires are impreganted with Epibond 100A. The assembly is next placed in a teflon mold and the diameter built up to somewhat greater than that finally desired. After the epoxy is cured the mold is removed and the outside diameter machined using the brass rod and pin for centering purposes. The piece is then fixed in a lathe by this machined surface. The brass rod and pin are bored out, and the inside and outside dimensions are finished as shown in Fig. 3. The measurements volume (I) is sealed onto the bottom of (G) using Epibond 121. A thin filter of cotton wool is placed over the upper end of the interconnecting hole (H), and CMN powder is packed into the upper volume. A 1/64 in. o.d. cupronickel He^3 filling tube is sealed into plug (F) with Epibond 100A. This plug in turn is sealed into (G) using Epibond 121. Plug (K) is sealed in last, with Epibond 121, so that one may test for continuity of the gas path.

The mechanical support between the measuring cell and the main refrigerator is made by means of a rod (N) of Epibond 100A. Thermal isolation is provided by boring out a section 45 mm long, 10 mm o.d., leaving a 1 mm wall.

To improve the thermal isolation of the He[3] two steps were taken, both of which are helpful First of all, the side walls of the cell are placed in thermal contact by means of copper wires (B) and (P) with a thermal guard consisting of a paste of 7.5 g of CMN powder and 4.6 g of 20,000 centistoke viscosity Dow-Corning "200" fluid [57]. The method of interleaving copper wires is shown in Fig. 3. A resistance thermometer, not shown in the figure, is placed in contact with this paste. The outside is covered with a mylar sheet to maintain a dry external surface. The second improvement resulted from covering the whole lower section of the apparatus with a thermal shield (L) consisting of three layers of coil-foil painted with the "Dag"-7031 mixture. Over the cell structure and the guard is wound a helix (M) of 0.02 in. diam thread which serves as thermal isolation from the shield (L). This shield is thermally grounded in the region (S) by means of coil-foils (B) at the temperature of the chrome alum (U). The upper end (Q) of the zinc switch (R) is connected to 3000, 0.002 in. diam Formex insulated copper wires in the form of 8 coil-foils 1/2 in. wide (B) which are placed in contact with the chrome alum as shown.

2. Coils and electronics

The field H_0 is produced by two circular coils located external to the nitrogen dewar. They were wound with 100 turns each of 0.102 in. diam heavy Formex insulated copper wire. The coils have an average diameter of 39.2 cm and an average separation of 25.4 cm. Departure from Helmholtz geometry was necessary because of a lack of space external to the cryostat. This set of coils produces a field at its center of 3.78 I gauss/amp. The resulting gradient along H_0 at a displacement from the geometrical center in the direction of H_0 of half the length of the measurement cell is $G_{H_0} = 1.1 \times 10^{-3} H_0$ cm^{-1}, giving a gradient of approximately 0.02 gauss/cm at a working field of 18.5 gauss. The current for these coils is supplied by a Kepco model KS-36-30M regulated DC supply, controlled remotely by two 10-turn potentiometers providing both a coarse and fine current control. The current is monitored by measuring the voltage developed across a 0.1 ohm shunt with an L and N type K-3 potentiometer. The intentional field gradient G is produced by a set of two coils with fields opposing. These are located on the outside of the helium dewar at liquid nitrogen temperature and with current elements as shown in Fig. 5. This coil design was developed here by H.R. Hart, Jr. For a homogeneous gradient one
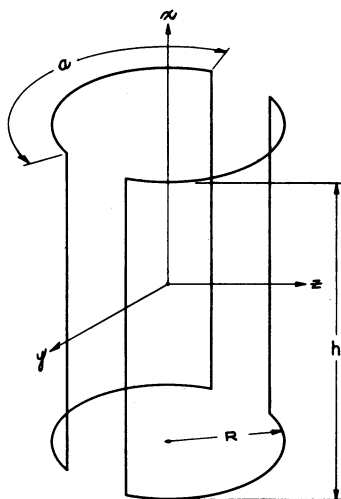

FIGURE 5

Geometry of coil for producing the homogeneous gradient.

has $a/R = 1.5998$, and $h/R = 1.9674$, giving for the gradient in the z direction at the center $G = 0.9858\ N\ I/R^2$ cm gauss/amp turn, where N is equal to the number of turns in each coil. In the present experiment, $R = 6.14$ cm, $N = 19$ turns, and $G = 0.497\ I$ gauss/cm amp. For this configuration, the first non-zero value of $(\partial^n G/\partial z^n)_{z=0}$ occurs for $n = 4$ [58].

The rf coil (W) which produces the field $2\ H_1$ has a single layer, 3.2 cm in diameter by 3.0 cm in length, containing 79 turns of 0.010 in. diam heavy Formex insulated copper wire. This coil gives a field at its center of $2\ H_1 = 22.6\ I$ gauss/amp. It is wound on a set of coil-foils (V), shaped as shown in Fig. 3. The coil-foils are electrically grounded, thus forming a Faraday shield, by a single copper wire soldered to the top of (V) and thermally grounded by greasing them to the inner surface of the He^4 shield (X) as shown. The weight of this structure is supported, at room temperature, by means of the lid (Y) which closes the He^4 shield and isolates the shield (X) from the bath at 4°K by means of a nylon spacer (Z).

The mutual inductance coils are geometrically similar to those already described for the specific heat experiment (part C of Sec. III). The only difference is that the number of secondary turns is reduced to 1087 per coil, the number of turns per tap remaining the same. Although these coils are located nearly over the rf coils, no spurious ringing or pickup is observed.

The current for the pulse coil is supplied by a gated amplifier following a General Radio type 805C signal generator. Pulses and timing are provided by Tektronix series 160 pulse and waveform generators. The amplifiers are the same as those used previously. All of the circuitry is described in the pa.er of Anderson, Reese, and Wheatley [21] and in even more detail in the thesis of Reese [59]. An LC filter with a Q of about 50, placed between the final amplifier and a Type 531 Tektronix oscilloscope, serves to increase the ratio of signal to noise.

In a spin-echo measurement of D, one requires a 90° and a 180° pulse with a fixed short interval between them followed by a second 180° pulse at a variable time. The 90° pulse is selected to be approximately 300 μsec long, for which case there are enough cycles to avoid significant frequency spread in spite of the random starting phase [60]. The corresponding value for $2\ H_1$ is approximately 0.5 gauss. The gradient G is gated off during each pulse since it would lead to a variation of H_0 across the sample which is of the same order of magnitude as H_1, and hence would not allow proper pulsing.

After tuning the pickup coil and the LC filter to the frequency of the signal generator, the spin echo equipment is tuned as follows. The field $2\ H_1$ is set approximately by adjusting the pulse current to the calculated value corresponding to the pulse width. Then, the amplitude of the free induction decay following a 90° pulse is photographed, measured, and plotted as a function of the current which produced the field H_0. The field H_0 is then set according to these measurements. The pulse current is then varied, both pulse current and free induction decay being recorded photographically, and that pulse current is selected which gives the maximum amplitude of the free induction decay. The pulse current and H_0 now having been fixed, the 180° pulse width is obtained by recording photographically the free induction decay amplitude following a single pulse of nearly 180°. That pulse width is selected which corresponds to zero amplitude for the free induction decay. Following these adjustments the whole electronic apparatus, which is supplied by a stabilized a.c. line, is very stable for many days, neither the pulse electronics nor the amplifiers changing by more than a few percent.

In the frequency range for these measurements we were annoyed by a spurious signal in the range of 50 to 75 kc/sec which was not entirely stable in frequency. It is hypothesized that this signal came from the rf high voltage power supplies for the oscilloscopes. It was also necessary to be very careful concerning grounds so as to avoid pickup of power line frequencies.

The time standard for the experiments is a Tektronix Type 180-A time-mark generator. The gains of the amplifiers were measured by comparing a signal sent simultaneously to the oscilloscope and to the input of the amplifier chain, appropriately attenuated so as to produce about the same signal on the oscilloscope in both cases. Absolute comparison was made possible by means of the calibrating signal in the oscilloscope.

The residual gradient at the measurement cell was estimated from the first zero occurring in the free induction decay in zero applied gradient to be approximately 0.02 gauss/cm. This value is that expected from the inhomogeneity in the H_0 field.

E. Execution of Experiment

Immediately after the first transfer of liquid He^4 into the main bath, but before any He^4 is admitted into the He^4 evaporator, the calibration of the magnetic thermometer is made. Some He^3 gas is allowed to enter the cell, but the valve in the He^3 line is then closed, for otherwise the readings drift as the He^3 slowly condenses. Calibration is effected by pumping down the main bath and measuring the mutual inductance of the measuring coils as a function of $1/T$, T being obtained from the vapor pressure of the liquid He^4. Calibration is made over a range of $1/T$ from 0.46 to 0.9°K^{-1}. About 200 μ of He^4 exchange gas is used. Calibration points usually fall on a straight line with less than 1 per cent scatter.

At least once for each apparatus the mutual inductance vs $1/T$ was measured with the demagnetization apparatus still at liquid nitrogen temperature. At times some residual magnetism has been found in such an experiment. It usually is eliminated on installing new mutual inductance coils or in some other way cleaning up that section of the apparatus. This problem is no doubt connected with some sort of magnetic impurity which is introduced inadvertently near the measuring coil.

After completing the magnetic calibration the main bath is returned to atmospheric pressure and the He^4 exchange gas is pumped out. Electrical heaters of about 200 ohms are located on the chrome alum, the ferric alum, and the He^3 evaporator. One and one-half to three volts is applied to each heater and the residual He^4 exchange gas pressure in the apparatus is monitored by means of a Veeco MS9/A mass spectrometer leak detector. When the leak rate goes below a certain value, which has been determined empirically, the heaters are turned off. By this time the temperature of the demagnetization apparatus is around 10°K.

He^4 is now admitted to the He^4 evaporator and pumped down to 1°K. He^3 is condensed and allowed to enter the He^3 evaporator so that the process of cooling the adiabatic demagnetization apparatus begins. Within approximately half an hour the demagnetization apparatus is below 2°K. At this time the main solenoid and the CMN solenoid are positioned, and the main solenoid is brought up to full field and left in the persistent-current mode. The He^3 refrigerator continues to cool the apparatus. So much refrigeration is required during the early stages of the magnetization that it is necessary for someone continuously to stand by the He^3 needle valve to admit He^3 to the system. Near 1°K the cell is filled with He^3 by means of a glass gas-handling system. Once the temperature has dropped below about 0.8°K the heat extraction rate is sufficiently slow that the apparatus may be left for long periods of time. The magnetization is continued until the temperature is reduced to approximately 0.28°K. This process requires from 12 to 18 hr. No He^3 is admitted to the evaporator during the last several hours of the magnetization since near 0.3°K approximately one hour is required for the temperature of the apparatus to recover fully following admission of He^3. We wish to emphasize that it is important to wait for the magnetizing temperature to be lowered to as small a value as is

possible. Following magnetization the first stage adiabatic demagnetization begins. It is important to make this demagnetization isentropic. For this reason the field is reduced in small steps, waiting a sufficient length of time for quasi-equilibrium, and progress is continually monitored with resistance thermometers attached to the chrome alum and the cell. The schedule usually followed is shown in Table 3. This schedule was obtained empirically by stepping the current through a small value, by observing the time for thermal equilibrium, and then by

TABLE 3

Demagnetization schedule for main solenoid

From	T_0	Time interval
15000 gauss	10000 gauss	0.4 hr
10000	5000^a/	2.3
5000	2500	2.7
2500	1000	4.0
1000	500	4.5
500	200	3.0
200	0	2.0
	Remain at 0	7.0
	Total	25.9 hr

a After reaching 5000 gauss the field in the CMN solenoid is established
at 2700 gauss.

shortening these times as much as possible. The final waiting period of approximately seven hours is important. A shorter period leads to a more rapid initial warm-up after a demagnetization of the second stage and probably corresponds to a higher temperature before second stage demagnetization. The effect of a shorter waiting period will be shown in the discussion of the heat capacity experiment. The small-step demagnetization procedure is based on the general result that the irreversible increase in entropy, ΔS_i, of two bodies which are placed in thermal contact with an initial temperature difference $\Delta T \ll T$ is related to ΔS, the absolute value of the concomitant change of entropy in either body, by the relation $\Delta S_i/\Delta S \approx \Delta T/T$. In the present work, $\Delta T/T$ is kept less than about 10 per cent except at very low temperatures where the He^3 entropy is much less than that of the chrome alum.

The schedule for the second stage demagnetization by the CMN solenoid is shown in Table 4. That schedule was arranged after considering the equilibrium times in the heat capacity experiment at various temperatures. The thermodynamic efficiency of the final demagnetization can be estimated if the temperature just prior to demagnetization can be estimated and if an entropy-temperature curve for CMN in zero field is available. In the heat capacity experiments the

TABLE 4

Demagnetization schedule for CMN solenoid

From	To	Time interval
2700 gauss	1800 gauss	11 min
1800	900	15
900	580	10
580	360	10
360	220	12
220	140	11
140	70	11
70	0	7
	Total	1 hr 27 min

temperature at which the apparent residual heat leak is zero corresponds to approximately 14 m°K. Assuming this to be the temperature of the chrome alum one assumes a slightly larger starting temperature of approximately 15 m°K. One also assumes that $S/nR = 0.01$ initially for the CMN, that $S_{He3} = 7 \times 10^6 \ TV$ erg/cm^3°K^2 as determined in the present experiment, and that the $S-T$ relation for CMN is that given by de Klerk [31]. For the final temperature one takes the lowest temperature for which there appears to be thermal equilibrium. This is about 4 m°K in the case of the heat capacity cell, that temperature being reached about 30 min after demagnetization (it is possible that a lower temperature would be more appropriate in this case). In the case of the diffusion cell one takes the final temperature to be 3.4 m°K (on the diffusion temperature scale) corresponding to about 10 to 15 min after demagnetization. Correcting this temperature to $H_0 = 0$ would give a temperature after demagnetization to zero field of about 3.2 m°K. From these figures an estimate has been made of the entropy of the CMN and the He^3 before and after demagnetization. The results are shown in summary in Table 5. The thermodynamic efficiency could be improved but probably not before the residual heat leak is substantially reduced. In terms of thermodynamic efficiency better results were obtained with the heat capacity cell than with the diffusion cell. This probably resulted from the longer thermal time constants in the diffusion cell due to the appendix of He^3 and due to the tighter packing of CMN. The greatest loss probably occurred in the region of 10 to 15 m°K.

The residual heat leak in the heat capacity experiment, when no zinc switch was used, was typically 0.035 erg/sec. Better results were obtained in the apparatus for magnetic measurements when the residual heat leak was about 0.02 erg/sec.

Both in the heat capacity and magnetic properties apparatus it is possible to make an experimental estimate of the time required to attain thermal equilibrium once an intial temperature

TABLE 5

Thermodynamic analysis of He^3-CMN cooling. T_i and T_f are the initial and final temperatures S_i and S_f are the initial and final entropies

Cell	Mass$_{CMN}$ (g)	V_{He^3} (cm^3)	T_i (m°K)	$S_{i_{He^3}}$ (10^{4}erg/°K)	$S_{i_{CMN}}$ (10^{4}erg/°K)	S_i (10^{4}erg/°K)	T_f (m°K)	$S_{f_{He^3}}$ (10^{4}erg/°K)	$S_{f_{CMN}}$ (10^{4}erg/°K)	S_f (10^{4}erg/°K)	S_i/S_f
Heat capacity	1.55	.676	15	7.1	0.2	7.3	4.0	1.9	8.4	10.3	.71
Diffusion	4.11	1.15	15	12.1	0.4	12.5	3.2	2.6	17.9	20.5	.61

inhomogeneity has been established. In the heat capacity case the variation of indicated CMN temperature with time during and following a heating period is analyzed. In the magnetic case the initial temperature inhomogeneity is produced by a step change in the external field H_0. The resulting, estimated, thermal time constants, τ are then analyzed to give a thermal resistance on the basis of a two bath model for which $\tau = RC_3C_{CMN}(C_3 + C_{CMN})^{-1}$, where R is the thermal resistance at the surface of and inside the CMN crystals, C_{CMN} is the heat capacity of the CMN powder, and C_3 is the heat capacity of the He^3. Any reasonable estimate of the thermal relaxation time of the He^3 itself leads to the conclusion that for all practical purposes the He^3 is at a uniform temperature, even when it is heated non-uniformly. The results are surprising. First of all, the values of R obtained in Runs 1 and 2 of the heat capacity experiment, corrected for the difference in quantity of CMN, agree with those obtained with the magnetic measurements cell. Other values of R from the heat capacity experiment, corresponding to the runs which took place after a low temperature purging of the cell, are about a factor 2 less. The values of R vary approximately as $T^{-0.7}$ between 5 m°K and 10 m°K, except for values from the purged cell which have an even weaker temperature dependence. At 5 m°K the estimated resistivity is about 30 times *less* than that for an epoxy-He^3 surface. Numerical values naturally depend on the accuracy of the estimate of the surface area of the powder, but the fact remains that the thermal resistance of the powder is remarkably low. At the least, this fact has considerable technical significance. The low thermal resistance between He^3 and CMN powder observed here may be a realization of the conditions tentatively suggested in Section II.

F. Purification of He^3

It is important to remove He^4 impurities from the liquid He^3 since they may serve as scattering centers for the He^3 quasiparticles. Actually, however, the He^3 should be self purifying due to the phase separation effect. A theory of this effect has been given by Edwards and Daunt [61] which successfully predicts the phase separation curve for He^3 fractions greater than 10 per cent, corresponding to the available experimental data. Subsequently Brewer and Keyston [62] found, in a partially filled cell of liquid He^3, a large heat leak which disappeared after the temperature of the cell had risen above 0.15°K. They interpret the heat leak in this partially filled cell as resulting from a film flow of He^4 which had separated from the non-superfluid He^3-He^4 mixture below the temperature of 0.15°K. In this laboratory we found, and interpreted qualitatively in a similar fashion, the same effect for a partially filled cell in one of our first experiments on self-diffusion in 1959. Brewer and Keyston find that their estimated He^4

impurity and the measured phase separation temperature are in reasonable agreement with the formula of Edwards and Daunt, $Y = 1.13\ T^{3/2}\exp(-0.71°K/T)$, where Y is the concentration of He^4 in the He^3-rich or upper phase at the temperature T. This formula predicts $Y = 30 \times 10^{-6}$ at 0.1°K, and $Y = 0.009 \times 10^{-6}$ at 0.05°K, so that it seems very unlikely that there would be any appreciable He^4 impurity unseparated in the millidegree range. However, because of the possible nuisance value of He^4 and the possible, though not probable because of phase separation, intrinsically serious effect of He^4 as a scatterer, we have made a substantial purification of our He^3 and tested the effect of input gas purity on the heat capacity.

Several years ago a rectifying column was built in this laboratory along the lines suggested by Peshkov and Zinov'eva [63], but scaled down in size so that the quantity of He^3 in the column was not large. This column is 4 in. long, 3/16 in. in diameter, and packed with rings 0.022 in. in diameter made from 0.002 in. diam nickel wire. This column works satisfactorily down to He^4 impurities of about 15 to 30 parts per million (ppm), but not well below that. The first heat capacity data were obtained with He^3 purified in this way. The purification limit of the column is determined at least in part by the requirement that for small quantities of He^4 impurity the column will work properly only if the temperature difference across the column is less than $\Delta T = 0.4c°K$, where c is the concentration of He^4 at the bottom. For $c = 30$ ppm, one has $\Delta T \approx 12 \times 10^{-6}°K$.

Most purity measurements can be made using a Veeco MS9/A leak detector to measure He^4/He^3 ratios. A simple modification of the Veeco electronics allows He^3 measurements to be made. This modification consists of opening the lead between the "ion voltage" control, which is approximately at the potential of the final grounded electrode in the ion acceleration system, and of inserting three series connected 45 volt batteries in series with a potentiometer. This allows variation of the d.c. potential between the final electrode and the shield around the ion source from about 264 volts for He^4, to about 348 volts for He^3. A voltmeter is installed to indicate this potential difference so that the He^3 and He^4 peaks can be located easily. A switch added to the front panel alternately inserts the batteries in the circuit or removes them to establish the original wiring. This arrangement serves for quantitative measurements of the ratio of He^4 to He^3 down to 30 ppm as checked with a Consolidated-Nier mass spectrometer. The limiting sensitivity is about 10 ppm with an accuracy of about 50 per cent. Attempts to increase the sensitivity were unsuccessful.

Starting with a purity of 15 to 20 ppm a first attempt at further purification was made by a process of repeated partial evaporation. A He^3 refrigerator system was modified so that the evaporator would hold about 10 cm^3 of liquid. The evaporator was made of copper and a heater was wrapped around the outside near the bottom. The evaporated He was removed using the He^3 pumping system and the sample purity was determined using the Veeco by setting the He^3 signal at a maximum position and then tuning for He^4. There was no pressure dependent He^3 background at the voltage corresponding to the He^4 peak so long as the pressure in the system was kept below that value which corresponded to maximum reading for the He^3. When the gas was removed at an evaporator temperature of around 0.4 to 0.5°K very erratic behavior was observed. It was concluded that, in spite of the copper surroundings, substantial temperature differences occurred in the He^3 due to a lack of convective mixing, the heater being improperly located and the expansion coefficient of the He^3 in this temperature range being negative. A subsequent run at 0.6 to 0.7°K did not exhibit erratic behavior. From the work of Peshkov and Zinov'eva [63] one expects an improvement in the impurity of the gas which is initially removed by about a factor of 3. The actual results for the initial gas removed were much better, about a factor of 5 or 6 being obtained in the case where the He^3 was evaporated at a temperature of 0.6 to 0.7°K. If about 50 per cent of the gas originally condensed into the evaporator was removed, the He^4 impurity in the gas removed decreased by about a factor of 2. Starting with about 16 liters of gas at standard temperature and pressure and containing about 15 ppm of He^4, we found that

after 3 fractional distillations, in which in each case half the input gas was removed, that the final He^4 impurity in the last two liter fraction was (2 ± 1) ppm.

Since it seemed that some rectifying-column action was occurring in the copper evaporator just mentioned, it occurred to us that a rectifying column for He^3 containing only very small quantities of He^4 impurity might be constructed of a single copper tube packed transversely with copper screen. In such an arrangement it would be difficult, with the copper shell and with relatively rapidly refluxing He^3, to obtain a large temperature difference across the column. This is just the condition which is desirable for rectifying-column action in nearly pure He^3. Largely through the efforts of W.R. Roach such a column was built and tested. The apparatus, shown in Fig. 6, was soldered to the bottom of the existing He^3 evaporator in the
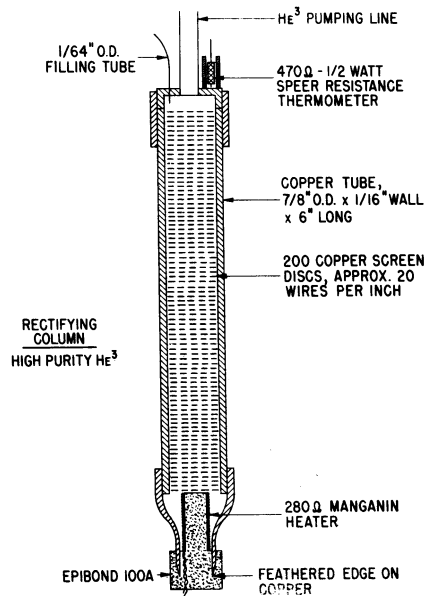
FIGURE 6

Rectifying volumn for producing high purity He^3.

He^3 refrigeration system. The column was operated with a power input of about 2 mW, and 3.5 l./hr gas were removed. The heating rate corresponds to an evaporation rate of He^3 of about 7 l./hr so that there is not a great deal of refluxing in the column as operated. Under typical operation, the resistance thermometer at the top of the evaporator corresponded to a temperature of 0.62°K, a temperature for which the expansion coefficient of He^3 is greater than zero, and the pressure at the inlet to the pumps was about 800 microns. The initial charge, which consisted typically of about 15 to 18 l. gas at standard temperature and pressure, was condensed into the column. The first portion removed was recirculated to purge the lines. He^3 gas was then removed steadily as indicated above. Samples of the evaporating gas could be tested frequently for He^4 content, but it turned out empirically that just as the He^4 content of the evolving gas started to increase, both the indicated temperature and the pressure at the inlet to the pumps increased rapidly. The valves in the system could be closed rapidly so that the recently removed impure gas was not accumulated with the purified gas. Some performance data of this column are as follows: Starting with the He^4 impurity at 73 ppm and removing 87 per cent of gas, it was found that in the gas removed the He^4 impurity had been reduced by a factor of 40. Starting with about 17 ppm He^4 and removing 99 per cent of the gas, an improvement of a factor of 3 to 4 was obtained. A similar improvement was obtained starting at 5 ppm and removing

93 per cent of the gas. One sees that a very substantial improvement over simple evaporation from a small evaporator has been obtained using this method. The apparatus has the advantage that it is capable of handling very large quantities of conventionally purified gas simply and that after several purifications the He^4 impurity in over 80 per cent of the initial gas may be reduced to about 1 ppm.

IV. HEAT CAPACITY MEASUREMENTS

All the heat capacity data obtained with the two heat capacity cells are shown in Fig. 7. One can see at a glance that the data for each cell are consistent and reproducible. In particular, one sees that there are no peculiar phenomena occurring below 7 m°K. One also sees that
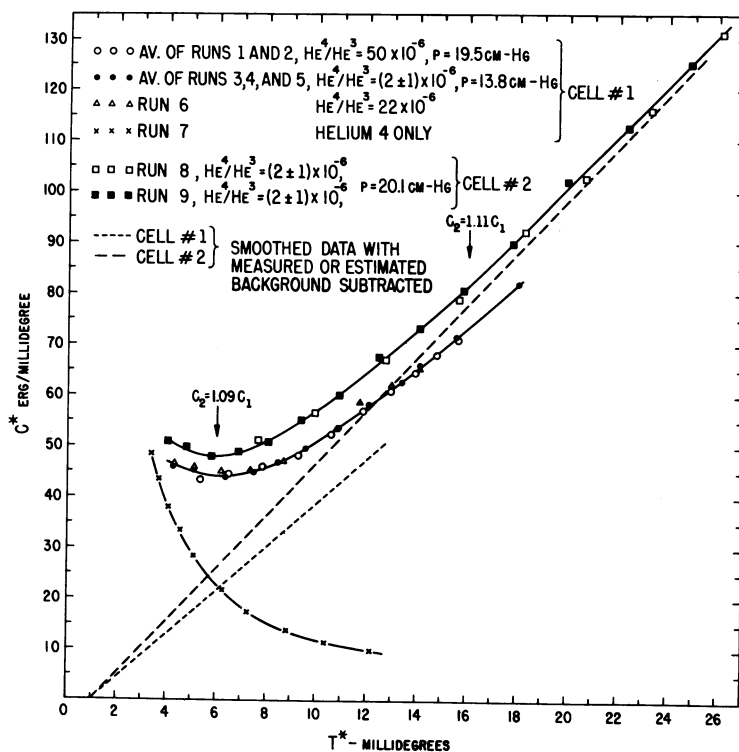
FIGURE 7

Collected heat capacity data.

there is no effect of He^4 impurity in the input gas extending from impurities of (2 ± 1) ppm to 50 ppm.

The reproducibility and consistency of the experimental data below 8 m°K are quite remarkable when one considers the raw data, an example of which in the region of 5 m°K is given in Fig. 8. In this figure the reading F of the mutual inductance bridge $[\Delta F \propto \Delta(1/T^*)]$ vs time (sec) after final demagnetization is shown for two different runs. These are typical of the "worst" conditions from which heat capacity data were obtained. The time in which heat is supplied by the heater is small compared with the time for the full temperature difference produced by that heat to develop in the thermometer. Moreover, the temperature difference produced
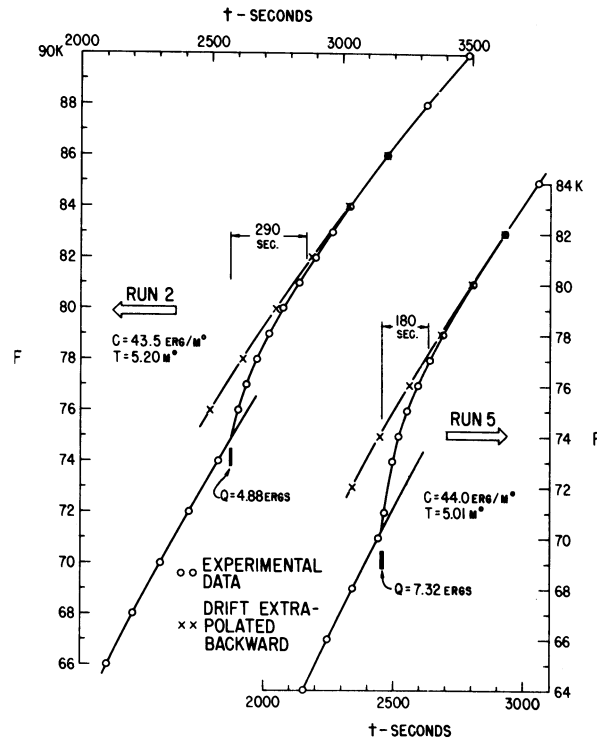
FIGURE 8

Examples of experimental heat capacity data in which mutual inductance bridge
reading, *F*, is plotted against the time after demagnetization, *t*.

by the residual heat leak is comparable to that produced by the externally supplied heat over
the interval of time required for dynamic equilibrium again to be produced. Assuming that the
drift curves as extended backwards in Fig. 8 are correctly drawn, one finds that in Run 2 the
equilibrium time is much longer than in Run 5. Between these two runs the 50 ppm helium was
removed. The cell was pumped at a higher temperature, about −100°C; purged with dry nitrogen;
pumped out and purged with high purity He³; and then finally refilled with high purity He³.
The more rapid thermal equilibrium time was not due to purity since the subsequent Run 6 with
22 ppm of He⁴ also displayed short equilibrium times. The important point here is that the two
heat capacity measurements differ by a very different equilibrium time as well as by different
amounts of externally supplied heat, different lengths of time during which the heater is
turned on, and slightly different residual heat leaks. Yet the calculated heat capacities are
in good agreement.

Why good results are obtained under such "poor" conditions may be understood after one
studies the residual heating rate. The early work of Anderson, Salinger, Steyert, and Wheatley
[17] on the Kapitza resistance was done using a cell similar to the one used here. They found
agreement with experimental data on the assumption that the residual heat leak was given by the
expression

$$\dot{Q} = \Gamma T^*_{CrK}{}^4 \left[1 - (T^*_{CMN}/T^*_{CrK})^4\right], \tag{19}$$

where T^*_{CrK} is the magnetic temperature of the walls and T^*_{CMN} that of the He³ and the CMN

together. Γ was a constant for a given cell. If the residual heating rate were given by this equation in the present experiment, then the heat capacity C^* on the magnetic temperature scale of the CMN-He^3 mixture could be obtained from the temperature-time drift curve within a constant factor, Γ. That is,

$$\frac{C^*}{\Gamma} = \frac{T^*_{CrK}{}^4}{\dot{T}^*_{CMN}} \left[1 - \left(\frac{T^*_{CMN}}{T^*_{CrK}} \right)^4 \right], \tag{20}$$

where T^*_{CrK} is T^*_{CMN} such that $\dot{T}^*_{CMN} = 0$. Values of C^*/Γ vs T^*_{CMN} are given in Fig. 9 for the various runs on Cell 1. The general features of the measured C^* vs T^* curves shown in Fig. 7 are reproduced here. At the low temperature end the measured value of C^*/Γ, at least in the early runs, rises sharply with increasing T and is not reproducible from run to run. Since C^*/Γ is inversely proportional to the rate of change of temperature $\dot{T}^*$ of the CMN, this sharp rise
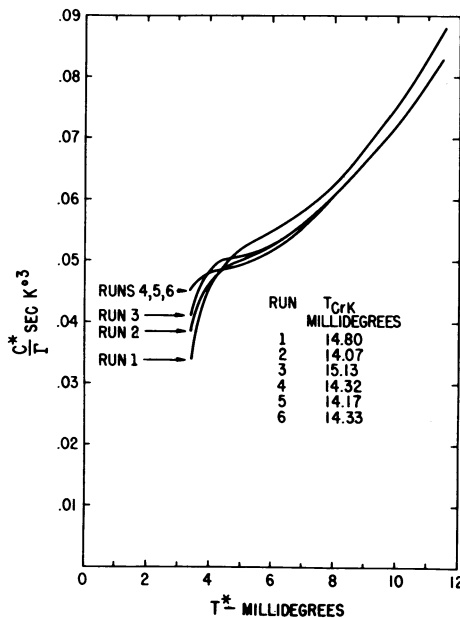
FIGURE 9

Effective heat capacity vs magnetic temperature as obtained from the zero
external power temperature-drift curves assuming the heat flow is
proportional to the difference in the fourth power of the temperatures
of the chrome alum (CrK) and the CMN.

corresponds to the initial transient before thermal equilibrium between the He^3 and CMN is established. As the runs proceeded and more experience was gained in performing the demagnetizations, the initial transients became less pronounced. This came as a result of two improvements in technique. First, in Runs 1, 2, 3, and 4 the period of time during which the demagnetization apparatus was left with the main field zero and the full field on the CMN successively increased from 1 or 2hr to about 7 or 8 hr. Second, the time of magnetization was increased so that the initial temperature before the first stage demagnetization was lower. From

these graphs one concludes that there was probably a reasonable thermal equilibrium for temperatures at least as low as 4.5 m°K. One also finds that above this temperature $C*/\Gamma$ is not dependent upon history and hence that the residual heat leak depends upon the temperature and not on the time.

Referring to Fig. 10, the residual heat input might result in a change of temperature with time as shown in Curve A. Let us call this curve the equilibrium drift curve. Since the residual heat input is not history dependent but depends only on temperature, the slope of the equilibrium drift curve depends only on the temperature and not on the time at which that temperature was attained. Now suppose that at a time t_i heat is introduced for a short period of time as in the present experiments. The indicated temperature will then follow a transient path, but after a certain time interval $(t_f - t_i)$ the equilibrium drift rate will again be attained. The subsequent curve of temperature vs time will be the same as Curve A except translated backward in time by a fixed time interval. Curve B on the figure is thus exactly the same
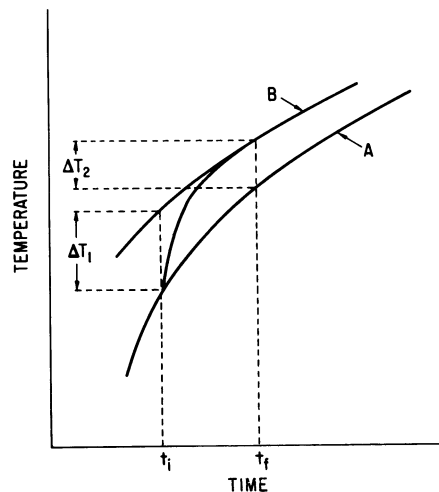
FIGURE 10

Possible experimental heat capacity data illustrating the uncertainty in the temperature difference produced by a certain amount of externally introduced heat.

as Curve A except that it has been translated backward in time by a fixed amount. Since the temperature difference for a given time between these two Curves A and B is not constant over the interval of time from t_i to t_f and since the indicated temperature is not necessarily the same as that of the He³, it is not obvious what temperature difference to take as that produced by the externally supplied heat unless the time interval $(t_f - t_i)$ is sufficiently short that the temperature difference produced by the externally supplied heat in this time interval is much greater than the temperature difference caused by the residual heat leak. There is, however, an important exception to this rule. If the heat flowing in through the walls is constant and if the heat capacity of the contents of the cell is also constant, then the equilibrium drift curves are straight lines and a good temperature difference can be obtained even when the equilibrium drift curve is rather steep. This is exactly the situation which obtains in the low temperature part of the present experiments. The residual heat leak is essentially independent of the temperature of the CMN as long as the CMN temperature is much less than the temperature of the walls. Moreover, it seems to be true empirically that the heat capacity of the present

cell in the range of temperatures between 4 and 8 or 9 m°K is nearly constant. Indeed on plotting temperature vs time for the equilibrium drift curve one finds nearly straight lines (± 2 per cent) over time intervals sufficiently long so that the temperature jumps produced by the externally supplied heat are well defined and not strongly affected either by the residual drift rate or by the internal equilibrium times in the cell.

Returning again to the treatment of the raw specific heat data, an equilibrium drift curve of $\dot{F}$ vs F was constructed from the measured curve of $\dot{F}$ vs F, the latter curve showing clearly at what F value the He³-CMN mixture was again in dynamic equilibrium following an externally applied heat pulse. Starting at a value of (F, t), following a heat pulse, such that dynamic equilibrium had again been established, the (F, t) curve was extended backward in time using the master $\dot{F}$ vs F curve and the relation $(F_2 - F_1) = \dot{F}(t_2 - t_1)$, where $\dot{F}$ is evaluated at $F = (F_1 + F_2)/2$. This method, when used to move forward in time, precisely predicted the measured points. In practice the ΔF used to compute the temperature change on applying heat was that corresponding to a time approximately at the midpoint of the transient although the calculated heat capacity did not depend strongly on what time was selected.

A survey of Fig. 7 shows that the ratio of the heat capacities of the two cells at any given temperature is nearly constant at about 1.1. Since the ratio of the mass of CMN to the total cell volume is essentially the same for the two cells, a linear scale factor applied to the specific heat should allow the data for one cell to be derived from the data for the other. Due to an error in construction of Cell 1, a small pocket not in good thermal contact with the main He³ volume was also filled with He³. This defect did not affect the heat capacity measurements but did make it impossible to measure the number of moles of He³ in the main He³ volume. Cell 2 did not possess this defect. It contained 0.0188 $\pm$ 1 per cent moles of He³.

Cell 2 was provided with a zinc thermal switch to disconnect it from the main refrigerator. Hence the heat capacity data for Cell 2 were carried to a substantially higher temperature than those for Cell 1, the latter being limited to an upper temperature just somewhat above the temperature of the chrome alum.

With Cell 1, one run was made with He⁴ instead of He³ in the cell. The results of the measurements are also shown in Fig. 7. The raw data had some rather distressing features. The curves of $\dot{F}$ vs time before and after a heating period did not join smoothly with one another. Moreover at higher temperatures, around 7 to 8 m°K, the heating produced distinct spikes on the F vs time curve. Both of these effects probably show a lack of thermal equilibrium, and the thermal spikes observed probably mean that some heat was lost to the surroundings due to momentary over-heating of the He⁴. This effect is not possible in the case of the He³ because of its higher heat capacity and higher thermal conductivity. Hence the data with only He⁴ in the cell may not be very meaningful. They do not obey a $1/T^{*2}$ law, but some departures, approximately a few erg/m°K might be expected because of the heat capacity of the heater, which might be similar to constantan or manganin for which evidence for an hfs heat capacity has been found [64].

In the case of Cell 2, no measurement of the background due to the CMN or the heater has been made, but above 15 m°K an approximate correction was made by subtracting the heat capacity of the CMN estimated as if it were given by [30] $CT^2/nR = 6 \times 10^{-6}$°K². Subtracting the "measured" background in the case of Cell 1 and the estimated background above 15 m°K in the case of Cell 2 and drawing the best straight lines through the results one finds the dashed curves shown in Fig. 7. The actual subtracted curve for Cell 1 falls below the dashed curve for temperatures below 5 to 6 m°K. The dashed curve for Cell 2 is based entirely on data above 15 m°K. The ratio of the slopes of the two dashed curves is 1.20 rather than the value 1.1 expected, as indicated earlier. Both extrapolate to zero at $T^* = 1$ m°K, as if $T = T^* - 1$ m°K. This result seems unlikely in view of the diffusion coefficient measurements to be described later.

Using the measured number of moles of He³ in Cell 2, (0.0188 ± 1 per cent) moles, and the upper dashed line, and putting $T = T^* - 1$ m°K, one finds $C_{He3}/nRT = 3.33$ °K^{-1}. This is about 15 per cent greater than the value given by Anderson, Reese, and Wheatley [65]. Assessment of the errors in the temperature scale and the measurement of the number of moles makes it appear unlikely that the discrepancy is due to either of these sources. There is a distressing lack of agreement with the measurements of Fairbank and co-workers [66] and of Brewer and Keyston [67] where the value of C/nRT is found to be between 2.2 and 2.3°K^{-1}.

A comparison with the older data of Anderson, Reese, and Wheatley and a re-examination of the present data above 15 m°K, making no assumptions either about the temperature dependence of the heat capacity of the He³ or about the background, is shown in Fig. 11 where the ratio C/nRT^* is plotted as a function of T^*, C being the total heat capacity and n the number of moles of He³ in the cell. One sees that in the older data the value C/nRT continues to increase as the
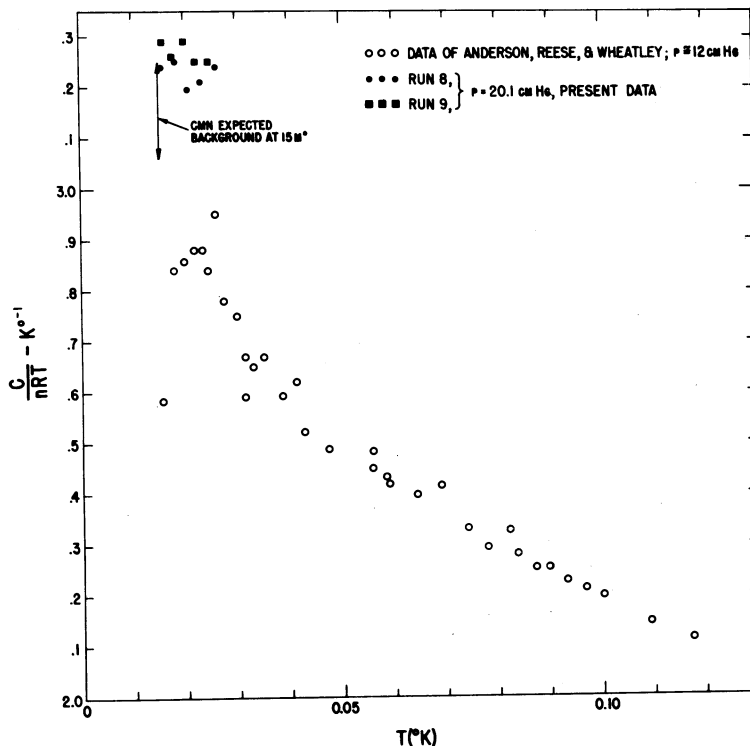
FIGURE 11

Collected data for C/nRT, where C is the total cell heat capacity vs magnetic temperature above 15 m°K. All data obtained in this laboratory for low pressure He³ are included.

temperature decreases. The new data are definitely higher than the old by about 10 per cent. The estimated background of the new data would subtract about 6 per cent from the C/nRT curve at 15 m°K, bringing it down to about 3.05 to 3.10 °K^{-1} at that temperature. Thus, from an experimental point of view the heat capacity of He³ is not definitely established to depend linearly on temperature even at 15 m°K, although the present value of C/nRT between 15 m°K and 25 m°K is much less dependent on temperature and less widely scattered than in the previous data. It might be remarked that the observed temperature dependence of C/nRT is not that predicted by Richards [68] on the basis of a finite temperature Fermi liquid theory. There still remains the possibility that there is a larger temperature dependent background than is

estimated here.

The present experiments also give some additional information on the Kapitza thermal boundary resistance phenomenon. From the curve of C^*/Γ, one can obtain Γ by putting in measured values of C^*. This procedure does not lead to a constant value for Γ. However, at 10 m°K one finds $\Gamma = 7 \times 10^5$ erg/sec °K^4 and, assuming that the entire inside wall area is effective in transferring heat, that $\Gamma/A = 10^5$ erg/sec cm^2°K^4. At 5 m°K Γ/A is 30 per cent greater than its value at 10 m°K. Assuming a cubic temperature dependence, this corresponds to a thermal resistivity $R = 2.5 \times 10^{-6}T^{-3}$ sec cm^2°K^4/erg for a He^3-epoxy interface. In the previous work of Anderson, Salinger, Steyert, and Wheatley [17], the numerical coefficient was found to be 3×10^{-6}.

During the run when He^4 was in Cell 1, an attempt was also made to measure the thermal boundary resistance. Comparing the curves of C^*/Γ for He^3 and He^4 at 7.3 m°K, one finds $R_4 \approx 2R_3$. In a single experiment in which the temperature difference produced by a constant, externally supplied heat flow was measured, it was found that for $\dot{Q} = 0.246$ erg/sec, the temperature changed from 14.7 m°K to 26.6 m°K, the average temperature being 20.7 m°K. This would correspond to $\dot{Q} = 5.4 \times 10^5$ $(T_{Hot}^4 - T_{Cold}^4)$ erg/sec °K^4. The corresponding numerical coefficient for the He^3 is 7×10^5 as mentioned in the preceding paragraph. Hence, for both of the above methods of estimating the Kapitza resistance between an epoxy wall and He^4 one finds $R_4 > R_3$ at temperatures less than 20 m°K, although in the He^4 measurements the thermal resistance of the bulk He^4 in the powder of CMN might not be negligible.

The above results may be compared with the work of Anderson, Connolly, and Wheatley [6], where the thermal boundary resistance between low pressure He^4 or He^3 and copper was measured down to 60 m°K. The ratio R_4/R_3 was always less than unity, but below 100 m°K the ratio was rapidly increasing with decreasing temperatures. It is possible then that the results from the two experiments are consistent, and that the ratio $R_4/R_3 > 1$ at temperatures lower than 20 m°K. Hence it may be, as discussed in Ref. 6, that at very low temperatures R_4 is approaching the value predicted theoretically by Khalatnikov [69] whereas R_3 remains 5.5 times less than the value recently calculated by Gavoret [22].

In view of the present work, the result of Peshkov [24] is perplexing. However, in light of the following discussion, we now believe his heat capacity peak to have been produced experimentally. For details of Peshkov's apparatus the reader is referred to his work. There are certain fundamental differences between his arrangement and ours. First, the ratio of the volume of He^3 to the mass of CMN refrigerant is, for us, 0.445 cm^3/g while for Peshkov it is 0.080 cm^3/g, there being 5.6 times less He^3 per unit mass of CMN in his experiments. For this reason he has substantially more refrigerating capacity and calorimeter background than in our experiment. Second, typical CMN grain size in our cell is 100 to 200 microns, while in Peshkov's cell the typical grain size is 10 microns. Third, the He^3 in our cell is heated by an internal heater located centrally in the loose powder where good internal thermal equilibrium is possible. We have never observed temperature spikes of any kind with the apparatus although a resistance thermometer is located in the He^3 so that any such temperature spikes would have been observed. The cell of Peshkov is heated either by means of an external electrical heater or by means of gamma rays. In both cases he observes temperature spikes on an external resistance thermometer on applying heat, although the temperature spikes are smaller in the case of gamma ray heating than in the case of electrical heating. Fourth, the temperature scale in our experiment is determined by calibrating the CMN between 1 and 2°K, and our CMN always remained at room temperature or below during the assembly of the apparatus. Peshkov's temperature scale is determined by assuming that the minimum magnetic temperature possible with CMN powder is 3.2 m°K, after the work of Daniels and Robinson [30]. Moreover, in the preparation of his cell, it is possible that the CMN is substantially above room temperature for short periods of time.

To understand Peshkov's results, consider a defect of his experiments which he points out in his paper. This defect is a heat loss. When a certain amount of heat Q is applied, a temperature change ΔT is measured. The calculated heat capacity is $C = Q/\Delta T$. But if some of the heat escapes, as for example up the mechanical support or the thermal switch, then Q in the equation for the measured heat capacity is too large, and the calculated heat capacity is too large. The greater the heat loss, the larger will be the apparent heat capacity.

Peshkov made several measurements with his cell. In one only liquid He^4 was introduced. The measured specific heat increased with decreasing temperature. Next, about 5 per cent of the volume was filled with He^3. He found the remarkable result that the heat capacity of the cell had decreased. The explanation was in terms of the "heat loss" phenomenon. It was assumed that the He^3 enabled the externally supplied heat to be more readily absorbed and hence reduced the overall heat loss so much that, in spite of the increased actual heat capacity, the calculated heat capacity was decreased. Next, the cell was filled completely with He^3 and curves of specific heat obtained which, with CMN heat capacity subtracted, were on the average in agreement with those of Anderson, Salinger, Steyert, and Wheatley [17] at higher temperatures. We note that the latter work was later found to be somewhat incorrect due to an error introduced by spurious magnetic materials in the calibration of the thermometer [70]. That is, the high temperature portion of Peshkov's data corresponds on the average to a value of C/nRT which is about a factor 4/3 less than the value given by the present measurements. At lower temperatures a bump appeared on the heat capacity curve, the bump being much larger for electrical heating than for gamma ray heating. There was heat loss also in the case of the completely filled cell and the amount of heat lost was estimated by the rather arbitrary procedure of forcing the heat capacity of the He^3 to be zero at 3.5 m°K.

Granted that heat loss exists, all that is required to produce a bump on the heat capacity curve is to have more heat lost in the region of the bump than in neighboring regions. Thinking of the process in terms of thermal time constants, if the time constant for equilibrium of the CMN-He^3 mixture goes through a maximum near 5 to 6 m°K, then more time will be available for heat to escape during the thermal spike which occurs during the heating period and the measured heat capacity will appear to have a bump on it. Using the two-bath thermal resistance formula for the time constant, $\tau = RC_1C_2/(C_1 + C_2)$, where C_1 might refer to the He^3 and C_2 to the CMN, we find for our cell that R seems to vary in the range of 5 to 10 m°K somewhat less strongly than T^{-1}, whereas on the basis of the Kapitza resistance we expected it to vary as T^{-3}. The product $C_1C_2/(C_1 + C_2)$ varies as T at low T and as T^{-2} at high T, peaking at a temperature where C_1 is approximately equal to C_2. Thus RC might be expected to peak at a temperature lower than that for which the heat capacities are equal. This is what is found by Peshkov. Since the peak in heat capacity observed by Peshkov when adding heat electrically is much greater than the gamma ray heating peak, and since thermal spikes were observed in both cases, we conclude that the peak is produced by some mechanism similar to the one described here and not by some fundamental property of the sample.

The good contact between the He^3 and the grains of CMN found by Peshkov corresponds, we believe, to a small thermal boundary resistance, as observed by us, and not to any phenomenon of superfluidity.

So far as thermometry is concerned, we feel that it is possible that Peshkov's procedure for calibrating his thermometer may also be in error. It is based on the assumption that for a sphere of CMN powder the minimum possible magnetic temperature is 3.2 m°K. This assumption is based on Daniels and Robinson's experiment with a single crystal ellipsoid. It is not obvious that in the powder of this highly anisotropic salt, whose interactions are largely dipolar, that the maximum susceptibility is the same as that in a single crystal, the g-factors being appropriately corrected for. Now suppose that $T^*_p = fT^*_t$, where T^*_p is Peshkov's assumed magnetic

temperature and T^*_t is the true magnetic temperature, and f is a factor. Then one finds that the ture ratio C/nRT is f^2 times as great as the value measured by Peshkov at higher temperatures. We have noted that according to our present work, one has $f^2 = 4/3$, while according to Refs. 66 or 67 $f^2 \approx 1$. Hence if Peshkov's temperature scale were calibrated by his heat capacity measurements near 10 m°K, the temperature quoted by him for the transition to superfluidity would remain unchanged, according to Refs. 66 or 67, or might be as low as 4.8 m°K, according to the present work. In either case the temperature is still substantially above the 4 m°K lower limit of the heat capacity measurements and the 3.5 m°K lower limit of the magnetic measurements to be described. It might also be noted that our lowest T^* for the heat capacity measurements was 1.99 m°K, and for the magnetic measurements was 3.17 m°K, in a field of 18.5 gauss. In neither case was the cell in internal equilibrium.

V. DIFFUSION, SUSCEPTIBILITY, AND SPIN-LATTICE RELAXATION TIME MEASUREMENTS

For the interpretation of spin-echo measurements in He^3 the reader is referred to the paper by Anderson, Reese, and Wheatley [21]. The important point is that the ratio of the amplitude of successive echoes is given by equation (18). Using the experimental data and this equation, D may be calculated. In the present work T_2 processes do not attenuate the echoes appreciably in the time intervals considered. The nuclear susceptibility χ may be measured on a relative basis simply by not applying G. A simple free induction decay may be enough to measure χ if the residual gradients are sufficiently small. However, one closely spaced echo is better, for then one can measure the actual maximum of the signal.

In the present measurements the temperature drift was slower than ever before and the increased ratio of CMN to He^3 in the magnetic measurement cell, compared with the specific heat cell, gave a lower temperature so that it was possible to make measurements at temperatures less than 4 m°K for over an hour and below 10 m°K for over 12 hr. Data on D and χ were obtained principally from two runs. The first was made at a He^3 pressure of 26.8 cm-Hg and the second at 14.6 cm-Hg. In both runs the impurity of the input gas was (2 ± 1) ppm He^4.

Measurements of χ and D are made alternately with T^* measurements interspersed from time to time. The a.c. magnetic measuring field for the CMN seriously affects the echoes and also causes some heating, the latter being observed for the first time in any of our cells. A D measurement consists of five photographs with G parallel to H_0 and five with G antiparallel to H_0. In some cases there is a difference in D between the two directions of the gradient, but in most there is no systematic difference. The signal to noise ratio is poorer in these experiments than in any previous ones and hence the quality of the data is not as good as before.

The echo heights and separation are obtained directly from the photographs by measuring with a scale having divisions every 0.02 in. The echoes can be bisected with an accuracy of a few thousandths of an inch, corresponding to at least 1 per cent accuracy for the time measurements. The height measurements are more difficult both because of the effect of noise and because of lack of definition of the oscilloscope trace. The time base of the oscilloscope is linear to an accuracy of better than 1 per cent over the region where the echoes occur.

Most of the photographs are rather lightly exposed to give more precision to the reading process. Fortunately some are suitable to demonstrate the type and quality of the experimental data. In Fig. 12 is shown a simple free induction decay at 3.45 m°K with zero gradient, frequency of 60 kc/sec, and external field 18.5 gauss. This is the lowest temperature photographed. There are 10 msec per major division seen on the photograph. The heating phenomenon is caused

by residual field gradients at the cell and corresponds to a gradient of about 20 milligauss per cm. The 90° pulse occurs at the end of the left-hand trace. The blank spot corresponds to
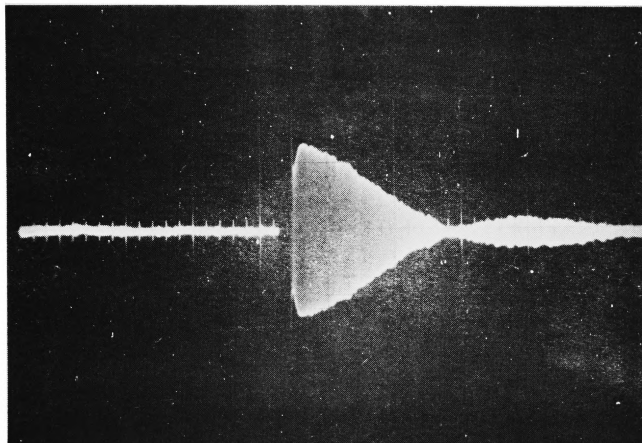

FIGURE 12

Free induction decay of liquid He^3 at 3.45 m°K in a static field of 18.5 gauss and zero externally applied gradient. The sweep is 10 msec/major division. This photograph was obtained at the lowest He^3 temperature attained in the present experiments.

the time interval in which the amplifier is saturated following the pulse. The free precession signal as photographed starts smaller than its peak value and builds up quickly. This must be some type of beating effect with other tuned circuits in the amplifier train. This effect goes away at higher temperatures. In Fig. 13 is shown a typical photograph used for measuring the susceptibility. This photograph was taken at a temperature of 4.1 m°K, with no external
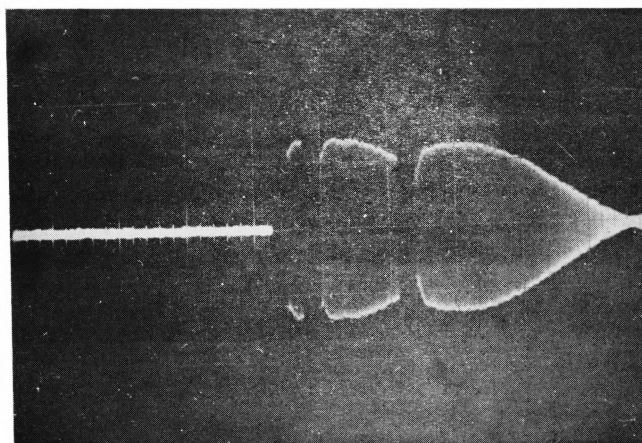
FIGURE 13

Typical photograph used for measuring relative nuclear susceptibility; $T = 4.1$ m°K. Two added 180° pulses distinguish this photograph from that in Figure 12.

gradient Proceeding from left to right, the blank spots mark the 90° pulse, the first 180° pulse, and the second 180° pulse. The relative susceptibility is obtained from the amplitude of the signal following the first 180° pulse. There are 10 msec per major division. One sees by comparing the amplitudes of the first and second echoes that there is very little diffusion attenuation in the time interval involved. In Fig. 14 are typical data for self-diffusion. This
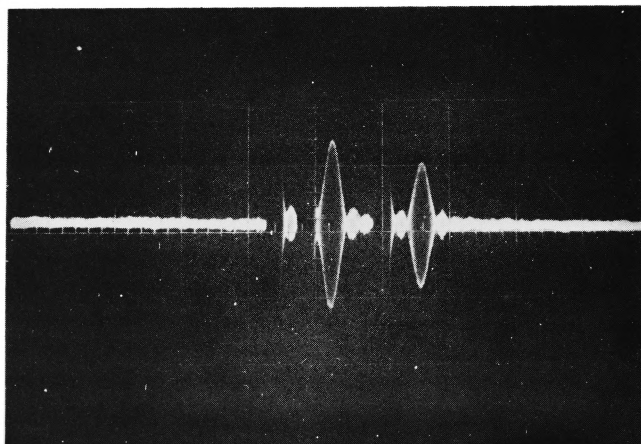

FIGURE 14

Typical photograph used for measuring the spin diffusion coefficient; $T = 4.0$ m°K. An externally applied gradient of 0.199 gauss/cm, applied parallel to the static field, distinguishes this photograph from that in Fig. 13. The attenuation of the second echo with respect to the first is due to the self-diffusion of the He³.

photograph was taken at a temperature of 4.0 m°K with an externally applied gradient of 0.199 gauss/cm. There are 10 msec per major division. The blank spaces on the trace are due to the 90° pulse and the two 180° pulses. The beats are due to the $(\gamma Gat)^{-1} \sin(\gamma Gat)$ type of beating of the signals from the various parts of the cell. The attenuation of the second echo is due to self-diffusion.

One finds that a plot of $\ln(h_2/h_1)$ is proportional to $(t_2 - t_1)^3$ within experimental scatter. The intercept of this straight line at low temperatures is typically 0.95 rather than 1. This is thought to be an experimental effect and was also found in all previous work. The graph of $\ln D$ and $\ln \chi$ vs $\ln T^*$ is shown in Fig. 15. One sees that the data fit a law $1/T^{*2}$ fairly well, though close examination shows that this law is not as precisely defined as in the work of Anderson, Reese, Sarwinski, and Wheatley [20]. Examination of the relative susceptibility curve as a function of T^* shows that this quantity gradually decreases, as the temperature drops from 30 m°K to about 3.5 m°K, the total drop being about 6 per cent. An effect of this sort had been seen in previous experiments and thought to be of essentially experimental origin. It is now believed that the effect is caused by the slight shift, equation (17), in the total steady field H_0 at the site of the measuring cell due to the dipolar field from the CMN. As mentioned in Section III, part D-1, for the geometry and mass of CMN in the present cell, there is produced at the site of the measuring cell at a temperature of 4 m°K an incremental field opposed to the externally applied field H_0 and of magnitude $2.2 \times 10^{-3} H_0$ due to the CMN. As mentioned in Section III, part D-2, during the process of tuning the spin-echo apparatus a curve of free induction decay amplitude is plotted as a function of the applied field H_0. The

tuning process is done at a temperature of 100 to 200 m°K. One finds from examination of the amplitude vs H_0 curve that if at high temperatures the field H_0 is located exactly on resonance a fractional change of 2.2 x 10^{-3} in this field will cause the amplitude to decrease by 4 to 6 per cent. This is about the same as the decrease observed in the measured relative suscepti- bility. Since the drop has roughly the right dependence on temperature as well, one concludes that the drop in relative susceptibility with decreasing temperature is in fact experimental.
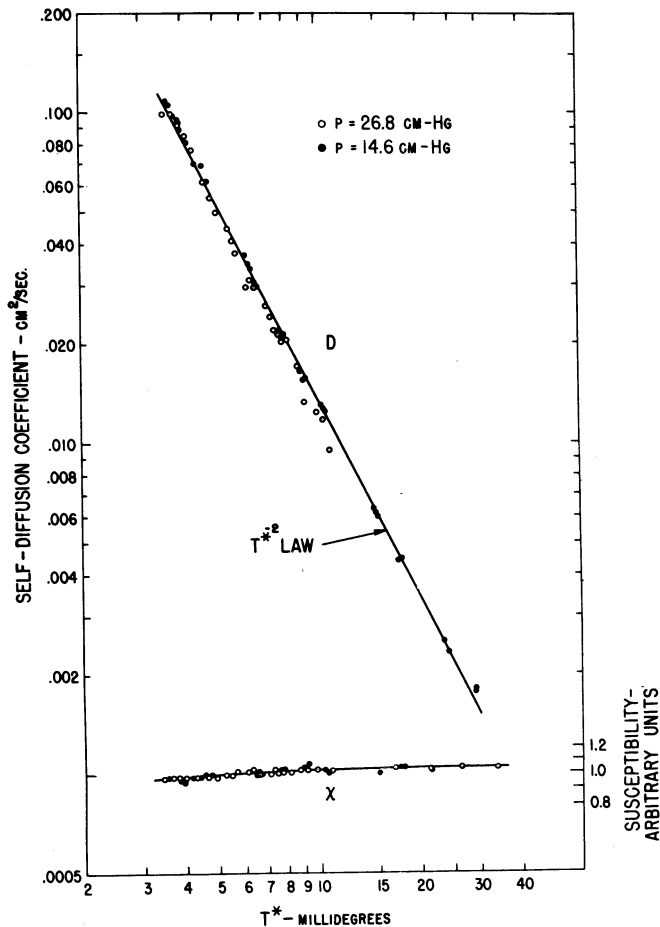
FIGURE 15

Self-diffusion coefficient and susceptibility of liquid He^3 at low pressure vs magnetic temperature.

Measurements at high temperatures than about 10 m°K are more questionable in this apparatus, which was basically designed to function at that temperature and below. Recalling that the thermal time constant of the appendix is approximately 300 $(T/10$ m°K)^2 sec and that the ratio of the thermal resistance of the He^3 column to the thermal resistance of the surrounding wall is 2 x 10$^{-2}(T/10$ m°K)^4, one finds that while at 10 m°K it is reasonable to expect good contact between the He^3 in the CMN region and the He^3 in the measuring region, at 20 m°K this is not at all as good an approximation. In fact, considerable difficulty was experienced in obtaining thermal equilibrium at temperature much above 15 m°K; although, in the run with a pressure of 14.6 cm-Hg where conditions were unusually good, it was possible to get adequate experimental data except at the very highest temperature of around 30 m°K.

If one writes $D = A/T^2$, then $A = 1.36 \times 10^{-6}$ cm^2°K^2/sec in the present experiments, while in the experiments of Anderson, Reese, Sarwinski, and Wheatley [20] the corresponding coefficient was 1.54×10^{-6} at about the same pressure. We have no explanation for the difference between these two coefficients.

The present measurements may be interpreted as a measurement of the relative susceptibility as a function of the diffusion coefficient with T^* being only a parameter used to correlate data. If the data are interpreted in this sense, there could arise no question concerning thermal equilibrium as perhaps might be raised in a criticism of the specific heat experiment. It is likely, however, that in the excellent conditions prevailing in the present experiments below 10 m°K there is no question of lack of thermal equilibrium between the CMN powder and the He^3 measuring cell. In the experimental data there is evident neither a sharp drop in the diffusion coefficient nor a drop in the susceptibility such as would be expected according to
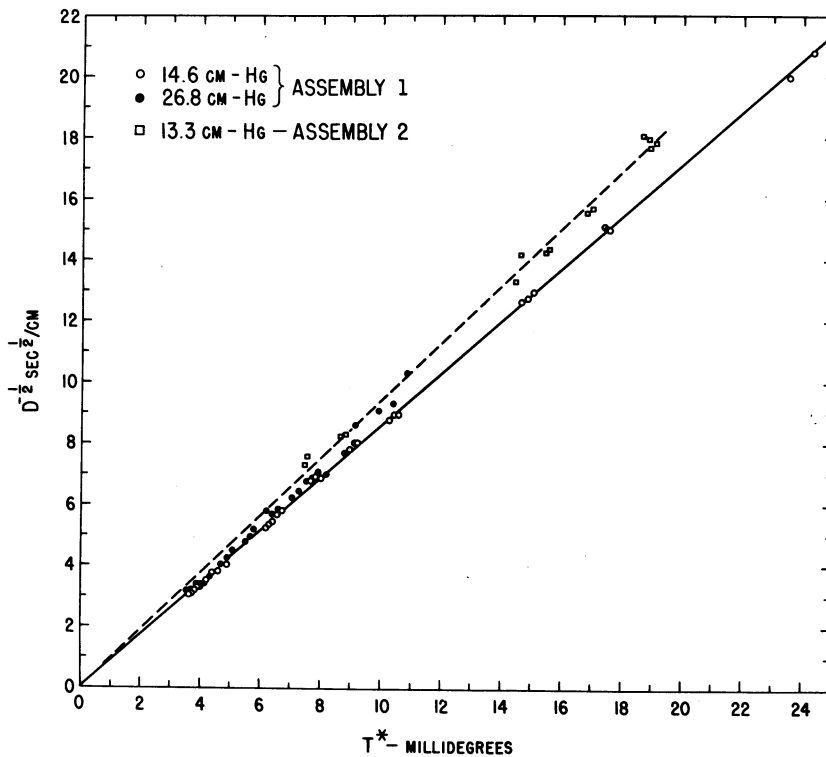

FIGURE 16

Inverse square-root of the diffusion coefficient of low pressure
He^3 vs magnetic temperature.

theories of superfluidity in He^3. Indeed, the data follow reasonably well a law $D = A/T^{*2}$ to the lowest temperatures. Hence one concludes from these data as well as from the specific heat data that above 3.5 m°K there is no transition to a superfluid state in He^3 at low pressure.

According to the Fermi liquid theory, the diffusion coefficient should be proportional to $1/T^2$, where T is the Kelvin temperature. Hence the Kelvin temperature should be proportional to the inverse square-root of the diffusion coefficient. In Fig. 16 we have plotted $D^{-\frac{1}{2}}$ vs T^*. The initial purpose of this plot was to see if $T = T^* - \Delta$, Δ being a shape dependent

constant frequently found in experiments on CMN for non-spherical samples. The best straight line through the experimental data at high temperatures passes through the origin. That is, it appears that $\Delta = 0$. This result is to be compared with the result of the heat capacity measurements where it was found that, if the specific heat of the He³ were forced to be linear below a temperature of 25 m°K, one would have $T = T^* - 1$ m°K. Hence, as discussed in the previous section, the assumption that the specific heat is linear in T below 25 m°K may not be precise. At the low temperature end one finds from Fig. 16 that T and T^* differ systematically by about 0.1 m°K, T being less than T^*. This difference would be in agreement with the analysis of de Klerk [31], although scatter of the experimental data does not allow a precise comparison.

Temperatures determined from $T \propto D^{-1/2}$ may represent only an upper limit to the actual temperatures, for any scattering mechanism in addition to quasiparticle scattering will reduce D from its $1/T^2$ value. Hence the lowest temperature of the present experiments is *at most* 3.5 m°K.

Also plotted in Fig. 16 are a number of experimental data for the diffusion coefficient obtained in a run made for the purpose of measuring the spin-lattice relaxation time in which diffusion measurements were incidental. The apparatus had been disassembled and reassembled before this run was made. These results for $D^{-1/2}$ at a given temperature lie definitely higher than those of the previous work, corresponding to a lower diffusion coefficient. We do not have an explanation for this discrepancy. However, we had been having trouble in this rerun with plugs forming in the filling tube and it is not inconceivable that there might have been an excess pressure in the cell. All the pulse parameters and resonance parameters on tuning the electronics were the same as before, and it seems impossible that G could be in error. The thermometer calibration was carefully rechecked and it was also rechecked that there were no spurious magnetic materials near the coils. There may have been some difficulty because of an increased residual heating rate, which was much greater than usual on this run because of a vibrational heat leak coming from a centering device which was being tested.

In the runs in which D and χ were measured it was noted that at very low temperatures the spin-lattice relaxation time T_1 became quite small, of the order of seconds. Hence, a separate run was made to make a preliminary study of this quantity. The method used is as follows: A pulse train is employed consisting of a 180° pulse followed at a variable time by a 90° and then a 180° pulse in quick succession with fixed small time separation. The first 180° pulse inverts the magnetization. The magnetization subsequently recovers, in the case of a purely exponential recovery, according to the formula

$$M_z = M_0 \left[1 - 2 \exp(-t/T_1) \right], \tag{21}$$

where M_0 is the equilibrium magnetization along z, the direction of H_0. In particular $M_z = 0$ when $t = T_{1/2} = T_1 \ln 2$. In the experiment, measurements are made alternately of $T_{1/2}$ and T^*. A typical photograph which illustrates the method is shown in Fig. 17. For each measurement of $T_{1/2}$ nine separate magnetizations are made with a magnetization time greater than 5 T_1 in each case. This particular photograph corresponds to $T^* = 8.1$ m°K and 1/2 sec per major division as the time base. The interval from the left-hand side of the sweep to the beginning of the echo is the time measured. Only part of the 90° free induction decay and the echo are visible on the photograph. The echo amplitude and the time interval are measured with a scale and plotted on linear paper. $T_{1/2}$ can be determined readily to a few per cent. Extending the amplitude curve back to zero time it is possible to find the quantity proportional to M_0 and test the exponential recovery. Departures from the exponential law are generally no more than a few per cent. A curve of $T_{1/2}$ vs T^* is shown in Fig. 18. It seems likely that the decrease of $T_{1/2}$ with decreasing T^* is connected with the rapidly increasing value of the self-diffusion
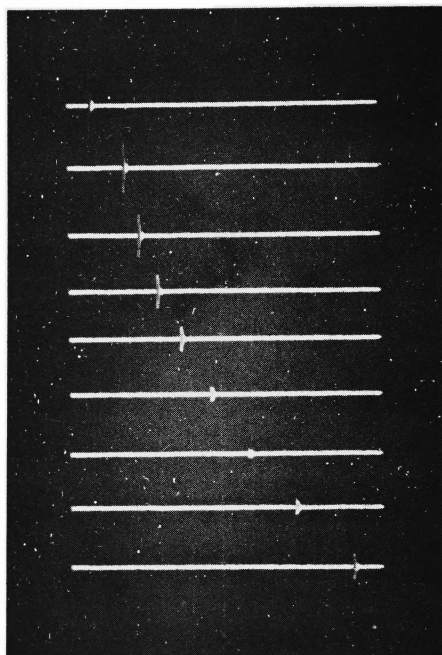
FIGURE 17

Typical photograph used for measuring spin-lattice relaxation; $T = 8.1$ m°K.
The sequence of nine sweeps illustrates the recovery of the magnetization
following a 180° pulse, which occurs at the extreme left-hand side of the
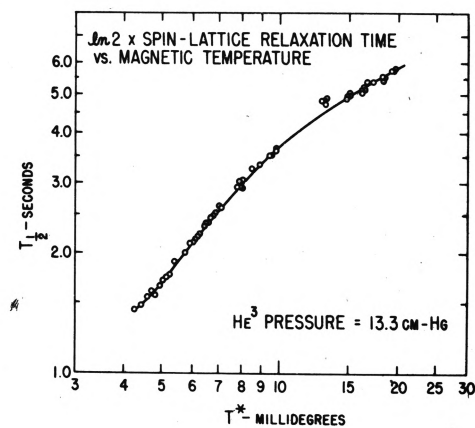trace. The full sweep is 5 sec.

FIGURE 18.

Time for the magnetization parallel to the static field
to reach zero following a 180° pulse, plotted against
magnetic temperature.

coefficient. Assuming that the nuclei are relaxed at the walls, most likely on the 8 x 8 mm faces, one might expect the time scale to be determined by the parameter l^2/D, where l is the half-height of the cell or 0.06 cm. At 5 m°K, $l^2/D = 0.06$ sec, while $T_1 = T_{1/2}/\ln 2 = 2.4$ sec, which is 40 times greater. Hence it appears that the walls are not at all black so far as relaxation is concerned. $T_{1/2}$ does not follow any simple temperature dependence.

It may turn out that T_1 will be a good thermometric parameter in a temperature range much lower than the present one. As the temperature drops, the self-diffusion coefficient becomes increasingly difficult to measure since smaller and smaller field gradients must be used. Moreover, as the temperature drops the cell must become longer both in order to prevent wall effects on the diffusion and to keep the width of the echo small. On the other hand $T_{1/2}$ may be measured simply and with some precision. Hence an experiment in which the susceptibility is measured as a function of $T_{1/2}$ may be possible even in the case where it is difficult to measure D.

VI. CONCLUSIONS

From measurements of the susceptibility and diffusion coefficient one finds that there is no transition to a new phase in He³ at low pressure down to a temperature of about 3.5 m°K. From measurements of the heat capacity and spin-lattice relaxation time, one finds that the transition does not occur above 4 m°K. At the same time it appears that the $1/T^2$ law for the collision time in the Fermi liquid is valid to below 5 m°K. Measurement of other parameters, particularly of the thermal conductivity and the viscosity, would be particularly interesting in this temperature range and, using the present techniques, possible to perform. Moreover, the theory of superfluidity in He³ predicts [71] that the transition temperature is higher at higher pressures. Hence the present measurements should be carried out through the full range of pressures available in the liquid.

In the present experiments C/nRT for temperatures between 15 and 25 m°K is about 5 to 10 per cent greater than in previous measurements and nearly 50 per cent greater than the extrapolated results of other workers. The differences with other experiments may be connected with the background heat capacity which is always present in the type of specific heat cell used in the present measurements. It is possible to do a different experiment such that the background heat capacity may be subtracted out, and a definitive experiment in this area should be done.

Assuming that the diffusion coefficient may be used to establish the Kelvin temperature scale, one finds that for a right circular cylinder of powdered CMN, with diameter and height equal, that T^* is almost equal to the Kelvin temperature, the departure being of order 0.1 m°K at 3.5 m°K. Although one analysis of the specific heat data leads to an apparent constant difference between the Kelvin and magnetic temperatures of about 1 m°K, a detailed consideration of the temperature dependence of C/nRT indicates that this conclusion might not be justified. It appears that CMN may be useful for producing temperatures substantially less than the limiting value of 3 m°K which is commonly assumed for this substance. A study of the relation of T^* to T for CMN powder at even lower temperatures would therefore be very interesting indeed. Such an investigation might be made with a nuclear precession thermometer, which might be more readily accepted as a standard than one based on the inverse square-root of the diffusion coefficient of He³.

The present apparatus works well for the production and maintenance of temperatures down to 3.5 m°K. With minor modifications of technique, it should be suitable for producing sufficiently low temperatures for a conventional experiment on "zero sound". Moreover, the He³-CMN forms a thermal bath, including thermometer, which has a short time constant and is suitable for

performing experiments on other materials at these very low temperatures, for example on the properties of superconductors having very low transition temperatures.

The fact that the spin-lattice relaxation time is beginning to change more rapidly with decreasing temperatures is interesting and measurements of this phenomenon should be carried to lower temperatures. T_1 might be a better thermometric parameter at lower temperatures than D, which would be more difficult to measure because of its large magnitude.

Acknowledgments

References

1. L.D. LANDAU, *Zh. Eksp. Teor. Fiz.* **30**, 1058 (1956) [English transl.: *Soviet Phys. - JETP* **3**, 920 (1957)].

2. A.A. ABRIKOSOV and I.M. KHALATNIKOV, *Reports on Progress in Physics* (The Physical Society, London, 1959), Vol. 22, p. 329.

3. D. HONE, *Phys. Rev.* **121**, 669 (1961).

4. L.D. LANDAU, *Zh. Eksp. Teor. Fiz.* **32**, 59 (1957) [English transl.: *Soviet Phys. - JETP* **5**, 101 (1957)].

5. I.L. BEKAREVICH and I.M. KHALATNIKOV, *Zh. Eksp. Teor. Fiz.* **39**, 1699 (1960) [English transl.: *Soviet Phys. - JETP* **12**, 1187 (1961)].

6. A.C. ANDERSON, J.I. CONNOLLY, and J.C. WHEATLEY, *Phys. Rev.* **135**, A910 (1964).

7. B.E. KEEN, P.W. MATTHEWS, and J. WILKS, *Physics Letters* **5**, 5 (1963); B.E. KEEN and J. WILKS, *Proceedings of the Ninth International Conference on Low Temperatures Physics*, 1964 (to be published).

8. L.P. PITAEVSKII, *Zh. Eksp. Teor. Fiz.* **37**, 1794 (1959) [English transl.: *Soviet Phys. - JETP* **10**, 1267 (1960)].

9. K.A. BRUECKNER, T. SODA, P.W. ANDERSON, and P. MOREL, *Phys. Rev.* **118**, 1442 (1960).

10. V.J. EMERY and A.M. SESSLER, *Phys. Rev.* **119**, 43 (1960).

11. J. BARDEEN, L.N. COOPER, and J.R. SCHRIEFFER, *Phys. Rev.* **108**, 1175 (1957).

12. L.H. NOSANOW and R. VASUDEVAN, *Phys. Rev. Letters* **6**, 1 (1961).

13. P.W. ANDERSON and P. MOREL, *Phys. Rev.* **123**, 1911 (1961).

14. T. SODA and R. VASUDEVAN, *Phys. Rev.* **125**, 1484 (1962).

15. V.J. EMERY, *Ann. Phys.* **28**, 1 (1964).

16. R. BALIAN and N.R. WERTHAMER, *Phys. Rev.* **131**, 1553 (1963); A.V. SVIDZINSKII, *Dokl. Akad. Nauk SSSR* **153**, 1044 (1963) [English transl.: *Soviet Physics - Dokl.* **8**, 1197 (1964)].

17. A.C. ANDERSON, G.L. SALINGER, W.A. STEYERT, and J.C. WHEATLEY, *Phys. Rev. Letters* **6**, 331 (1961).

18. A.C. ANDERSON, G.L. SALINGER, and J.C. WHEATLEY, *Phys. Rev. Letters* **6**, 443 (1961).

19. W.R. ABEL, A.C. ANDERSON, and J.C. WHEATLEY, *Phys. Rev. Letters* **7**, 299 (1961).

20. A.C. ANDERSON, W. REESE, R.J. SARWINSKI, and J.C. WHEATLEY, *Phys. Rev. Letters* **7**, 220 (1961).

21. A.C. ANDERSON, W. REESE, and J.C. WHEATLEY, *Phys. Rev.* **127**, 671 (1962).

22. J. GAVORET, *Phys. Rev.* **137**, A721 (1965).

23. G.A. BROOKER, *Proceedings of the Ninth International Conference on Low Temperature Physics*, 1964 (to be published).

24. V.P. PESHKOV, *Zh. Eksp. Teor. Fiz.* **46**, 1510 (1964) [English transl.: *Soviet Phys. - JETP* **19**, 1023 (1964)]; *Proceedings of the Ninth International Conference on Low Temperature Physics*, 1964 (to be published).

25. A.C. ANDERSON, G.L. SALINGER, and J.C. WHEATLEY, *Rev. Sci. Instrum.* **32**, 1110 (1961).

26. J.I. CONNOLLY, W.R. ROACH, and R.E. SARWINSKI, to be published.

27. N. PHILLIPS, *Phys. Rev.* **134**, A385 (1964).

28. A.H. COOKE, H.J. DUFFUS, and W.P. WOLF, *Phil. Mag.* **44**, 623 (1953).

29. T.L. ESTLE, H.R. HART, Jr., and J.C. WHEATLEY, *Phys. Rev.* **112**, 1576 (1958).

30. J.M. DANIELS and F.N.H. ROBINSON, *Phil. Mag.* **44**, 630 (1953).

31. D. de KLERK, *Handbuch der Physik* (Springer-Verlag, Berlin, 1956), Vol. 15, p. 117.

32. R.P. HUDSON, R.S. KAESER, and H.E. RADFORD, *Proceedings of the Seventh International Conference on Low Temperature Physics* (University of Toronto Press, 1961), p. 100.

33. R.H. RUBY, H. BENOIT, and C.D. JEFFRIES, *Phys. Rev.* **127**, 51 (1962).

34. P.L. SCOTT and C.D. JEFFRIES, *Phys. Rev.* **127**, 32 (1962).

35. J.H. van VLECK, *Phys. Rev.* **59**, 724 (1941).

36. A.R. MIEDEMA and K.W. MESS, *Physica* **30**, 1849 (1964).

37. D.L. MILLS, *Phys. Rev.* **133**, A876 (1964).

38. F.R. NASH, *Phys. Rev. Letters* 7, 59 (1961).

39. Cryogenic Systems Department, Westinghouse Electric Corporation, Box 8606, Pittsburgh, Pennsylvania, 15221.

40. 30 pounds test braided nylon line No. 6030, South Bend Tackle Company, Chicago 45, Illinois.

41. Bentley-Harris Manufacturing Company, Conshohocken, Pennsylvania.

42. Furane Plastics, 4516 Brazil Street, Los Angeles, California.

43. "Coil-foil" consists of 30 layers of 0.002 in. diameter, heavy Formex insulated copper wire wound at 25 turns per inch on a large drum and painted with a mixture of toulene (25%), alcohol (25%), and G. E. 7031 varnish (50%).

44. A.C. ANDERSON, W. REESE, and J.C. WHEATLEY, *Rev. Sci. Instrum.* 34, 1386 (1963).

45. James E. Biddle Company, 1316 Arch Street, Philadelphia, Pennsylvania.

46. Speer Resistor Division, Speer Carbon Company, Bradford, Pennsylvania.

47. W.C. BLACK, Jr., W.R. ROACH, and J.C. WHEATLEY, *Rev. Sci. Instrum.* 35, 587 (1964).

48. J.C. WHEATLEY, *Rev. Sci. Instrum.* 35, 765 (1964).

49. Acheson Colloids Company, Port Huron, Michigan.

50. Federal Insulation Company, 549 West Randolph, Chicago, Illinois.

51. Wilbur B. Driver Company, 1875 McCarter Highway, Newark 4, New Jersey.

52. No. 21-1 Silver Print, G.C. Electronics Company, Rockford, Illinois.
Measurements by John I. Connolly of the susceptibility of this paint showed that in the helium range the temperature dependent susceptibility of 1 gm of paint was 0.19 of that for 1 gm of CMN. A resistor similar to the one used in the specific heat cell had a negative temperature dependent susceptibility equivalent in magnitude to 0.02 gm of CMN.

53. Crotronics Inc., West Main Street, High Bridge, New Jersey.

54. W.R. ABEL, A.C. ANDERSON, and J.C. WHEATLEY, *Rev. Sci. Instrum.* 35, 444 (1964).

55. H.Y CARR and E.M. PURCELL, *Phys. Rev.* 94, 630 (1954).

56. Rea Magnet Wire Company, East Pontiac Street, Fort Wayne, Indiana.

57. Electronics Products Division, Dow-Corning Corporation, Midland, Michigan.

58. A similar set of coils designed for a homogeneous field rather than gradient requires the values $a/R = 2.1077$, and $h/R = 3.3108$, leading to a field at the center of $H = 0.7544 \ NI/R$ gauss cm/amp turn. The first non-vanishing value for $\partial^n H_z/\partial z^n$ is for $n= 4$. An experimental measurement of a coil made to these specifications showed that H_z was within 1/2 per cent of its value at the origin at $(x/R, y/R, z/R)$ equal to $(0.35, 0, 0)$; $(0, 0.33, 0)$; and $(0, 0, 0.26)$; and within 1 per cent of its value at the origin at $(0.48, 0, 0)$; $(0, 0.37, 0)$; and $(0, 0, 0.32)$.

59. W. REESE, University of Illinois, Ph.D. thesis, 1962.

60. H.R. HART, Jr., University of Illinois, Ph.D. thesis, 1960.

61. D.O. EDWARDS and J.G. DAUNT, *Phys. Rev.* **124**, 640 (1961).

62. D.F. BREWER and J.R. G. KEYSTON, *Physics Letters* **1**, 5 (1962).

63. V.P. PESHKOV and K.N. ZINOV'EVA, *Reports on Progress in Physics* (The Physical Society, London, 1959), Vol. 22, p. 504.

64. J.C. HO, H.R. O'NEAL, and N.E. PHILLIPS, *Rev. Sci. Instrum.* **34**, 782 (1963).

65. A.C. ANDERSON, W. REESE, and J.C. WHEATLEY, *Phys. Rev.* **130**, 495 (1963).

66. M. STRONGIN, G.O. ZIMMERMAN, and H.A. FAIRBANK, *Phys. Rev.* **128**, 1983 (1962).

67. D.F. BREWER and J.R.G. KEYSTON, *Nature, Lond.* **191**, 1261 (1961).

68. P.M. RICHARDS, *Phys. Rev.* **132**, 1867 (1963).

69. I.M. KHALATNIKOV, *Zh. Eksp. Teor. Fiz.* **22**, 687 (1952).

70. A.C. ANDERSON, G.L. SALINGER, W.A. STEYERT, and J.C. WHEATLEY, *Phys. Rev. Letters* **7**, 295 (1961).

71. A.M. SESSLER, *Proceedings of the Second Symposium on Liquid and Solid Helium Three* (Ohio State University Press, Columbus, 1960), p. 81.